

**NASA CONTRACTOR
REPORT**



N 73-10322

NASA CR-2131

NASA CR-2131

**CASE FILE
COPY**

**ASSESSMENT OF A TRANSITIONAL
BOUNDARY LAYER THEORY AT
LOW HYPERSONIC MACH NUMBERS**

by S. J. Shamroth and H. McDonald

Prepared by

UNITED AIRCRAFT CORPORATION

East Hartford, Conn. 06108

for Langley Research Center

NATIONAL AERONAUTICS AND SPACE ADMINISTRATION • WASHINGTON, D. C. • NOVEMBER 1972

1. Report No. NASA CR-2131		2. Government Accession No.		3. Recipient's Catalog No.	
4. Title and Subtitle ASSESSMENT OF A TRANSITIONAL BOUNDARY LAYER THEORY AT LOW HYPERSONIC MACH NUMBERS				5. Report Date November 1972	
				6. Performing Organization Code	
7. Author(s) S. J. Shamroth and H. McDonald				8. Performing Organization Report No.	
9. Performing Organization Name and Address United Aircraft Corporation United Aircraft Research Laboratories East Hartford, CT 06108				10. Work Unit No.	
				11. Contract or Grant No. NAS1-10865	
12. Sponsoring Agency Name and Address National Aeronautics and Space Administration Washington, D.C. 20546				13. Type of Report and Period Covered Contractor Report	
				14. Sponsoring Agency Code	
15. Supplementary Notes					
16. Abstract <p>An investigation has been carried out to assess the accuracy of a transitional boundary layer theory in the low hypersonic Mach number regime. The theory is based upon the simultaneous numerical solution of the boundary layer partial differential equations for the mean motion and an integral form of the turbulence kinetic energy equation which controls the magnitude and development of the Reynolds stress. Comparisons with experimental data show the theory is capable of accurately predicting heat transfer and velocity profiles through the transitional regime and correctly predicts the effects of Mach number and wall cooling on transition Reynolds number. The procedure shows promise of predicting the initiation of transition for given free-stream disturbance levels. The effects on transition predictions of the pressure-dilatation term and of direct absorption of acoustic energy by the boundary layer have been evaluated.</p>					
17. Key Words (Suggested by Author(s)) Laminar, transitional, and turbulent compressible boundary layers. Prediction of transition location, transitional boundary layer profiles.				18. Distribution Statement Unclassified - Unlimited	
19. Security Classif. (of this report) Unclassified		20. Security Classif. (of this page) Unclassified		21. No. of Pages 68	
				22. Price* \$3.00	

ASSESSMENT OF A TRANSITIONAL BOUNDARY LAYER THEORY AT LOW HYPERSONIC MACH NUMBERS

S. J. Shamroth and H. McDonald
United Aircraft Research Laboratories

SUMMARY

This investigation assesses the accuracy of a transitional boundary layer theory in the low hypersonic Mach number regime. The theory, previously shown to be applicable to subsonic and moderately supersonic flows, is based upon a simultaneous solution of the integral turbulence kinetic energy equation and a finite-difference solution of the boundary layer partial differential equations of motion. The investigation reported here shows the capability of the original form of the theory to accurately predict Stanton numbers and mean velocity profiles through the transitional regime at low hypersonic Mach numbers and with a slight modification to correctly predict the effect of Mach number and wall cooling on transition Reynolds number. The procedure also shows promise of predicting initiation of transition for a given free-stream turbulence disturbance level; an accurate assessment of this capability, however, cannot be made until more detailed experimental data become available. An investigation of the direct effect of fluctuating pressure shows the pressure-dilatation contribution to the turbulence kinetic energy balance, usually ignored at low Mach numbers, has, at most, a moderate effect in the low hypersonic Mach number regime. In addition, transition calculations performed with the usual free-stream turbulence intensity source term set to zero and a magnitude ascribed to the turbulence source term representing the direct absorption of acoustic energy by the boundary layer show that to trigger transition requires only a small amount ($\approx 1\%$) of acoustic energy absorption.

INTRODUCTION

Transitional boundary layers play an important role in the successful design and operation of a hypersonic reentry vehicle. During transition both the wall shear and wall heating can reach their peak values, thus having a potentially important effect on vehicle drag and the amount of wall cooling required to maintain structural integrity. In addition, the wake structure behind the vehicle which depends upon

the wall boundary layer development may vary significantly with transition location. Thus an analytical procedure capable of predicting transitional hypersonic boundary layers would be a useful tool in vehicle design.

Presently, there exist three main approaches for developing a transitional boundary layer theory: the semiempirical approach, the stability theory approach, and the turbulence kinetic energy approach. Typical examples of the semiempirical approach for predicting transition location are discussed by Hairston (ref. 1). Semiempirical procedures cannot be used with confidence to predict transitional properties for flow conditions significantly different from the flow conditions of the correlating data. This uncertainty is further heightened by the effects of tunnel influence upon transition experiments. As shown by Pate and Schueler (ref. 2) and Pate (ref. 3), correlations based upon transition data from one tunnel do not necessarily correspond to correlations based upon data from a different tunnel. Therefore, tunnel effects may severely limit the validity of semiempirical theories and make them inapplicable to free-flight situations.

In addition to the drawbacks inherent in data correlations, most semiempirical theories make the crude assumption that transition occurs instantaneously. A more realistic transition model developed by Harris (ref. 4) still requires specification of both the location and extent of the transition region but does not assume instantaneous transition. In ref. 4 Harris assumes the transitional shear stress as a linear combination of the laminar shear stress and a fully-developed turbulent shear stress, the linear combination factor being a universal function of the dimensionless streamwise location within the transitional region adapted from the low speed correlation of Dhawan and Narashima (ref. 5). This model has successfully predicted the development of transitional boundary layers in the low hypersonic Mach number regime and represents a significant improvement over instantaneous transition models. However, since it heavily depends upon empiricism and was not intended to predict the effect of phenomena such as free-stream turbulence, Mach number, wall temperature, etc. upon transitional behavior, it does not serve as a general boundary layer transition prediction procedure.

The second possible approach which might lead to an analytical prediction of transitional boundary layers is based upon stability theory. In classical stability theory the flow is divided into a mean flow whose stability is the subject of the investigation and a superimposed disturbance of specified form. The resulting equations are simplified through the boundary layer assumptions, linearized with

respect to the disturbance flow field, and then solved to determine conditions for amplification of the disturbance. Attempts to predict the initiation of transition from classical stability theory (for example, ref. 6) have had only qualitative success and this approach has yet to be applied successfully to the problem of transitional boundary layer development. The neglect of nonlinear phenomena and the assumption of purely two-dimensional disturbances makes classical stability theory, without major modification, an unlikely method of predicting the behavior of transitional boundary layers.

The third approach for predicting the behavior of transitional boundary layers is based upon the solution of the turbulence kinetic energy equation. Whereas, stability theory in a sense extrapolates forward from laminar to turbulent flow, use of the turbulence kinetic energy equation is an effort to extrapolate backward from the turbulent to laminar regimes. Since the turbulence kinetic energy equation derives directly from the Navier-Stokes equations (e.g., ref. 7), with no further assumptions, it is fundamentally a more accurate mathematical description of the transition process than is the linearized two-dimensional disturbance equation (the Orr-Sommerfeld equation) used in classical stability theory. Obviously, a formal relationship must exist between a transition theory based upon the turbulence kinetic energy equation and classical stability analysis since the turbulence kinetic energy equation governs both the wave motion of stability theory and the developing turbulence.

The turbulence kinetic energy equation has proven to be a useful tool in predicting the behavior of a wide variety of turbulent boundary layers (e.g., refs. 8 and 9) and has been extended to the transitional regime by Glushko (ref. 10), Donaldson, Sullivan, and Yates (ref. 11), and McDonald and Fish (ref. 12). The approaches of refs. 10 through 12 are basically similar in philosophy: i.e., they integrate an equation (or, in the case of Donaldson, et al., a set of equations) governing the streamwise development of the turbulent shear stress; however, they differ in the relationships introduced to allow performance of the integration. At the present time, neither the work of Glushko (ref. 10) or Donaldson, et al. (ref. 11) has been developed into a practical prediction procedure although preliminary calculations by Beckwith and Bushnell (ref. 13) indicate that Glushko's method perhaps could be developed satisfactorily. The approach used by McDonald and Fish (ref. 12) has proven capable of accurately predicting the behavior of a wide variety of transitional boundary layers in the subsonic and low supersonic Mach number regimes. The present investigation assesses the ability of the theory of ref. 12 to predict the development of transitional boundary layers in the low hypersonic Mach number regime.

The existence of phenomena associated primarily with hypersonic flow makes a straightforward application of any existing low Mach number transitional boundary layer theory uncertain in the hypersonic flow regime. For example, in subsonic flow the free-stream turbulent kinetic energy, a vorticity disturbance mode, plays an important role in determining transition location (refs. 14 and 15). At high Mach numbers, in addition to the vorticity mode, disturbances take the form of sound modes (ref. 2) and entropy modes. The effect of the entropy mode upon transition location is thought to be small except perhaps at very high Mach numbers; however, as shown by Wagner, Maddalon, and Weinstein (ref. 16), even at high Mach numbers the entropy disturbance may remain small. On the other hand, even at moderately supersonic Mach numbers the acoustic mode may play an important role in determining transition location. A successful hypersonic transitional boundary layer theory has to relate the vorticity and the acoustic modes so that the vorticity fluctuation arising from the acoustic disturbance could be incorporated into the analysis and, in addition, allow for the direct absorption of acoustic energy. A second example of a phenomenon peculiar to high Mach number flows is the direct effect of fluctuating pressure terms upon the turbulent kinetic energy balance. At low Mach numbers these quantities are usually negligible, however, in the hypersonic regime they may be important. In the present investigation the applicability of the McDonald-Fish transitional boundary layer theory to the low hypersonic Mach number regime is assessed. In making the assessment, comparisons between theory and experiment including velocity profiles, Stanton numbers, and integral thickness parameters are made and the ability of the procedure to predict the initiation of transition is determined. In addition, a preliminary assessment of the direct role of the fluctuating pressure is made.

LIST OF SYMBOLS

A_n	nonlinear coefficients, (see Eq. (A-5))
a_n	structural coefficients of turbulence
B_n	nonlinear coefficients, (see Eq. (A-6))
C_p	specific heat
C_f	skin friction coefficient
D	sublayer damping factor

F	dimensionless stream function
G'	dimensionless temperature ratio
K	constant coefficient, (see Eq. (39))
k	thermal conductivity
L	dissipation length
ℓ	mixing length
ℓ_∞	wake value of mixing length
M	Mach number
M_r	Mach number relative to free stream
Pr	Prandtl number
Pr_τ	turbulent Prandtl number
P	pressure
Q	heat flux
$\overline{q^2}$	turbulence kinetic energy
r	radius
Re_x	Reynolds number based upon streamwise distance
R_τ	turbulence Reynolds number
\overline{R}_τ	layer averaged turbulence Reynolds number
R_θ	Reynolds number based upon momentum thickness
St	Stanton number
T	static temperature
T^0	total temperature
u	streamwise velocity
u_τ	friction velocity

v	transverse velocity
w	cross flow velocity
x	streamwise coordinate
y	transverse coordinate
y^+	dimensionless transverse coordinate
α	indicator equal to one for axisymmetric flow, zero for two-dimensional flow
β	density ratio
Γ	intermittency factor
γ	ratio of specific heats
δ	boundary layer thickness
δ_s	sublayer thickness
δ_{TH}	thermal boundary layer thickness
δ^*	displacement thickness
δ^+	reference length
ϵ	turbulence dissipation
η	dimensionless transverse coordinate
θ	momentum thickness
μ	viscosity
ν	kinematic viscosity
ν_T	kinematic eddy viscosity
ρ	density
τ	shear stress

ϕ_1, ϕ_2, ϕ_3 integral functions (see Eqs. (20) through (22))

Subscripts

- e boundary layer edge condition
- ∞ free-stream condition
- w wall condition

Superscripts

- average quantity
- ' fluctuating quantity

THEORY

The Basic Equations

Within the framework of boundary layer theory, various authors (for example, Schubauer and Tchen (ref. 17)) have reduced the time-averaged Navier-Stokes equations to the compressible boundary layer equations of motion. For two-dimensional or axisymmetric flows, steady in the mean, the boundary layer approximations to the momentum, energy, and continuity equation become

$$\bar{\rho} \bar{u} \frac{\partial \bar{u}}{\partial x} + \bar{\rho} \bar{v} \frac{\partial \bar{u}}{\partial y} = - \frac{d\bar{P}}{dx} + \frac{\partial \tau}{\partial y} \quad (1)$$

$$\bar{\rho} \bar{u} C_p \frac{\partial \bar{T}^o}{\partial x} + \bar{\rho} \bar{v} C_p \frac{\partial \bar{T}^o}{\partial y} = \frac{\partial}{\partial y} (Q + \bar{u} \tau) \quad (2)$$

$$\frac{\partial \bar{\rho} \bar{u} r^a}{\partial x} + \frac{\partial \bar{\rho} \bar{v} r^a}{\partial y} = 0 \quad (3)$$

where x and y are coordinates in the streamwise and transverse directions, u and v are velocity components in the x and y directions, ρ is density, P is pressure, C_p is specific heat, T^0 is total temperature, r is the radius of curvature for an axisymmetric body, and the exponent α is zero for two-dimensional flows and unity for axisymmetric flows. The effective shear stress, τ , and the effective heat transfer, Q , are defined as

$$\tau = \bar{\mu} \frac{\partial \bar{u}}{\partial y} - \bar{\rho} \overline{u'v'} \quad (4)$$

$$Q = \bar{k} \frac{\partial \bar{T}}{\partial y} - \bar{\rho} C_p \overline{v'T'} \quad (5)$$

where μ is viscosity, k is thermal conductivity, T is static temperature. In Eqs. (1) through (5) overbars indicate averaged quantities and primes indicate fluctuating quantities. The equations are valid for laminar, transitional, or turbulent flows; obviously, for laminar flows the primed quantities are zero. For turbulent and transitional boundary layers it is convenient to represent the contribution of the apparent turbulent stress, τ_T , to the total shear stress, τ , by an effective turbulent viscosity, ν_T , and similarly the turbulent contribution to the total heat flux, Q , is represented conveniently by an effective turbulent conductivity, k_T , such that

$$\bar{\rho} \nu_T \frac{\partial \bar{u}}{\partial y} = - \bar{\rho} \overline{u'v'} \quad (6)$$

$$k_T \frac{\partial \bar{T}}{\partial y} = - \bar{\rho} C_p \overline{v'T'} \quad (7)$$

The turbulent conductivity, k_T , is related to the turbulent viscosity, ν_T , by a turbulent Prandtl number, Pr_T , defined as

$$Pr_T = \bar{\rho} C_p \nu_T / k_T \quad (8)$$

and the boundary layer momentum and energy equations, Eqs. (1) and (2), become

$$\bar{\rho} \bar{u} \frac{\partial \bar{u}}{\partial x} + \bar{\rho} \bar{v} \frac{\partial \bar{u}}{\partial y} = - \frac{\partial \bar{P}}{\partial x} + \frac{\partial}{\partial y} \left\{ (\bar{\mu} + \bar{\rho} \nu_T) \frac{\partial \bar{u}}{\partial y} \right\} \quad (9)$$

$$\begin{aligned} \bar{\rho} \bar{u} \text{ cp } \frac{\partial \bar{T}^0}{\partial x} + \bar{\rho} \bar{v} \text{ cp } \frac{\partial \bar{T}^0}{\partial y} = \frac{\partial}{\partial y} \left\{ \left(\frac{\bar{\mu}}{\text{Pr}} + \frac{\bar{\rho} \nu_T}{\text{Pr}_T} \right) \text{ cp } \frac{\partial \bar{T}^0}{\partial y} \right\} \\ + \frac{\partial}{\partial y} \left\{ \left[\left(1 - \frac{1}{\text{Pr}} \right) \bar{\mu} + \left(1 - \frac{1}{\text{Pr}_T} \right) \bar{\rho} \nu_T \right] \bar{u} \frac{\partial \bar{u}}{\partial y} \right\} \end{aligned} \quad (10)$$

In deriving Eq. (10) use has been made of the definition of total temperature

$$T^0 = T + \frac{u^2}{2\text{cp}} \quad (11)$$

With the flow laminar, Eqs. (3), (9), and (10) are solved with $\nu_T = 0$ to determine the boundary layer development. If the flow is transitional or turbulent, it is necessary to model ν_T and Pr_T . The specification of the turbulent viscosity, ν_T , and the turbulent Prandtl number, Pr_T , is carried out through the turbulence model described in detail in the subsequent section.

After specification of the turbulent viscosity and Prandtl number, Eqs. (3), (9), and (10) are solved by first eliminating $\bar{\rho} \bar{v}$ from the momentum and energy equations by application of the continuity equation. When the streamwise static pressure distribution, $P(x)$, is specified, the momentum and energy equations, in conjunction with an equation of state and equations governing ν_T and Pr_T , form a closed set of nonlinear, parabolic, partial differential equations which can be solved upon specification of boundary conditions. The wall and free-stream boundary conditions employed in the solution are given by:

at the wall, $y = 0$

$$\bar{\rho} \bar{v} = (\bar{\rho} \bar{v})_w, u = 0, \bar{T}^0 = T_w \text{ or } \frac{\partial \bar{T}}{\partial y} = 0 \quad (12)$$

at the free-stream, $y \rightarrow \infty$

$$\bar{\rho} \bar{u} = \rho_e u_e$$

$$\bar{T}^0 = T_e^0 \quad (13)$$

The subscripts 'w' and 'e' denote wall and free-stream conditions, respectively. The initial conditions for the problem are set by specifying the initial boundary layer displacement thickness, δ^* , and assuming the initial development is similar in the dimensionless coordinate, η , where

$$\eta = \frac{y}{\delta^*} \quad (14)$$

The numerical procedure used to solve the governing momentum and energy equations is a Hartree-Womersley approach in which streamwise derivatives are replaced by finite differences, the coordinate normal to the wall is nondimensionalized, and a stream function introduced. The resulting momentum equation is a third order nonlinear ordinary differential equation in the transverse coordinate and the energy equation is a second order nonlinear ordinary differential equation in the same transverse coordinate. At each streamwise station the nonlinear coefficients of each equation are estimated from the solution at the previous station and the resulting linearized equations solved as two-point boundary value problems. The resulting solutions are used to obtain better estimates of the nonlinear coefficients and the entire process repeated until two successive solutions agree to within a specified tolerance. The chosen numerical procedure has three outstanding attributes vis-à-vis other available methods of solving the partial differential equations. First it has great flexibility in streamwise step size which follows from the Hartree-Womersley representation of the streamwise derivatives in conjunction with the choice of nondimensional coordinate system normal to the wall. Both very large and very small streamwise steps may be taken, making the procedure ideally suited for either laminar, transitional, or turbulent flow since each type of boundary layer usually demands a different choice of streamwise step size (in terms of boundary layer thicknesses). The second attribute follows from the use of an implicit finite-difference procedure to solve the boundary value problem normal to the wall. Not only does the use of the implicit procedure enlarge the range of streamwise step sizes which the program can handle but since a

diagonally dominant matrix is obtained, very fast matrix inversion procedures can be utilized. Furthermore, an implicit method more properly represents a parabolic differential equation and allows for a very flexible grid normal to the wall thereby enabling a large number of grid points to be taken in the sublayer region. It should be pointed out that in calculating transitional and turbulent boundary layers the present procedure does not fit an empirical profile between the wall and the edge of the sublayer but rather calculates the flow development in the sublayer regime from the full boundary layer equations of motion and, thus, can include the effects of wall bleed and roughness in a fundamental manner. The third attribute of the procedure arises from the treatment of the nonlinear terms in the equations of motion. In this regard it is recognized that although almost all finite-difference procedures represent a linearization of some sort, the iterative updating of the nonlinear terms in the quasilinear form of the equations of motion treated by the present procedure goes a considerable way to relieving the restrictions imposed by the linearization inherent in other methods, at least in the y -direction. APPENDIX A describes the solution procedure in detail.

The Turbulence Model

Fully-developed turbulence model. - The fully-developed turbulence model originally presented by McDonald and Camarata (ref. 9) for two-dimensional incompressible flow, forms the basis for the transitional turbulence model used in the McDonald-Fish transitional boundary layer theory and, therefore, at this juncture it is useful to describe the model in some detail. The fully-developed turbulence model, which is described in greater detail in ref. 12, is based upon a solution of the turbulence kinetic energy equation. The turbulence kinetic energy equation is a conservation equation derived from the Navier-Stokes equations by writing the instantaneous quantities as a sum of mean and fluctuating parts. The i^{th} Navier-Stokes momentum conservation equation ($i = 1, 2, 3$, referring to the three coordinate directions) is multiplied by the i^{th} component of fluctuating velocity and the average of the resulting three equations is taken. The three averaged equations are summed to obtain the turbulence kinetic energy equation. The derivation of the turbulence kinetic energy equation has been given by Favre (ref. 7) for compressible flow and approximated by Bradshaw and Ferris (ref. 8) to boundary layer flows; a derivation and discussion of the turbulence kinetic energy equation for hypersonic flow is given in APPENDIX B.

As shown in APPENDIX B, the boundary layer approximation to the turbulence kinetic energy equation is given by

$$\begin{aligned}
 & \underbrace{\frac{\partial}{\partial x} \left(\frac{1}{2} \bar{\rho} \bar{u} \bar{q}^2 \right)}_{\text{advection}} + \underbrace{\frac{\partial}{\partial y} \left(\frac{1}{2} \bar{\rho} \bar{v} \bar{q}^2 \right)}_{\text{production}} = - \bar{\rho} \overline{u'v'} \frac{\partial \bar{u}}{\partial y} \\
 & \underbrace{- \frac{\partial}{\partial y} \left(\bar{\rho}' \bar{v}' + \frac{1}{2} (\bar{\rho} \bar{v})' \bar{q}^2 \right)}_{\text{diffusion}} - \underbrace{\bar{\rho} \epsilon}_{\text{dissipation}} \\
 & \underbrace{- \bar{\rho} (\bar{u}'^2 - \bar{v}'^2) \frac{\partial \bar{u}}{\partial x}}_{\text{normal stress production}} + \underbrace{\bar{\rho}' \frac{\partial u'_i}{\partial x_i}}_{\text{pressure-dilatation}}
 \end{aligned} \tag{15}$$

All calculations reported in the investigation were made with the usual assumption of zero pressure-dilatation contribution to the energy balance (ref. 8) unless otherwise stated. The turbulence model is developed by integrating Eq. (15) with respect to y between the limits $y = 0$ and $y = \delta$ which leads to

$$\begin{aligned}
 \frac{1}{2} \frac{d}{dx} \int_0^\delta \bar{\rho} \bar{u} \bar{q}^2 dy &= \int_0^\delta - \bar{\rho} \overline{u'v'} \frac{\partial \bar{u}}{\partial y} dy - \int_0^\delta \bar{\rho} \epsilon dy \\
 &- \int_0^\delta \bar{\rho} (\bar{u}'^2 - \bar{v}'^2) \frac{\partial \bar{u}}{\partial x} dy + \int_0^\delta \bar{\rho}' \frac{\partial u'_i}{\partial x_i} dy + E
 \end{aligned} \tag{16}$$

where

$$E = \left[\frac{1}{2} \bar{q}^2 \left(\bar{\rho} \bar{u} \frac{\partial \delta}{\partial x} - \bar{\rho} \bar{v} \right) - \bar{\rho}' \bar{v}' + \frac{1}{2} (\bar{\rho} \bar{v})' \bar{q}^2 \right]_e \tag{17}$$

Following Townsend (ref. 18) and Bradshaw and Ferris (ref. 8) structural coefficients a_n and L are introduced, together with a mixing length ℓ ; these scales are defined as

$$\begin{aligned}
 -\overline{u'v'} &= a_1 \bar{q}^2, \quad \overline{u'^2} = a_2 \bar{q}^2, \quad \overline{v'^2} = a_3 \bar{q}^2, \\
 \overline{w'^2} &= (1 - a_2 - a_3) \bar{q}^2 \\
 \epsilon &= (-\overline{u'v'})^{3/2} / L, \quad (\overline{u'v'})^{1/2} = \ell \frac{\partial \bar{u}}{\partial y}
 \end{aligned} \tag{18}$$

For fully-developed turbulence the structural coefficients α_1 , α_2 , and α_3 are assumed constant having values 0.15, 0.50, and 0.20, respectively (refs. 9 and 19). As is discussed subsequently, α_1 becomes a variable in the transitional regime. Using Eq. (18), Eq. (17) is put in the form

$$\frac{d}{dx} \left(\frac{\phi_1 \rho_e u_e^3 \delta^+}{2\alpha_1} \right) = \rho_e u_e^3 \left(\phi_2 - \phi_3 + \frac{E}{\rho_e u_e^3} \right) + \int_0^{\delta} \overline{\rho' \frac{\partial u'_i}{\partial x_i}} dy \quad (19)$$

where

$$\phi_1 = \int_0^{\delta/\delta^+} \frac{\bar{\rho} \bar{u}}{\rho_e u_e} \left(\frac{L}{\delta^+} \frac{\partial \bar{u}/u_e}{\partial \eta} \right)^2 d\eta \quad (20)$$

$$\phi_2 = \int_0^{\delta/\delta^+} \frac{\bar{\rho}}{\rho_e} \left(\frac{L}{\delta^+} \right)^2 \left(\frac{\partial \bar{u}/u_e}{\partial \eta} \right)^3 \left(1 - \frac{L}{L} \right) d\eta \quad (21)$$

$$\phi_3 = \int_0^{\delta/\delta^+} \frac{\bar{\rho}}{\rho_e} \left(\frac{\alpha_2 - \alpha_3}{\alpha_1} \right) \left(\frac{L}{\delta^+} \frac{\partial \bar{u}/u_e}{\partial \eta} \right)^2 \frac{\delta}{u_e} \frac{\partial \bar{u}}{\partial x} d\eta \quad (22)$$

where η is a nondimensional transverse distance y/δ^+ , δ^+ is an arbitrary reference length, and δ the boundary layer thickness.

The left-hand side of Eq. (19) represents the streamwise rate of change of turbulence kinetic energy and is derived directly from the turbulence kinetic energy advection term. The term $\rho_e u_e^3 \phi_2$ represents the integral of turbulence production minus dissipation and $\rho_e u_e^3 \phi_3$ is the normal stress production. The terms designated by E are turbulent source terms resulting from disturbances imposed upon the boundary layer by the free stream. As shown in Eq. (17), E is the sum of two major contributions, the first $(q^2/2)(\bar{\rho} u \partial \delta / \partial x - \bar{\rho} \bar{v})$ representing the free-stream velocity disturbance (i.e., free-stream turbulence entrained by the boundary layer) and the second, $\bar{\rho}' \bar{v} + (\rho \bar{v})' q^2/2$, representing the direct absorption of acoustic energy. (This acoustic energy absorption term will be subsequently explained in some detail.) It is the strength of the source term E which dictates the transition location.

For fully-developed turbulent flow, as in ref. 9, L and ℓ are given by

$$\frac{L}{\delta} = 0.1 \tanh [\kappa y / (0.1 \delta)] \quad (23)$$

$$\frac{\ell}{\delta} = \frac{\ell_{\infty}}{\delta} \tanh [\kappa y / \ell_{\infty}] \quad (24)$$

where ℓ_{∞} is the "wake" value of the mixing length at any particular streamwise station. Although Eqs. (23) and (24) give accurate representations of ℓ and L through most of the turbulent boundary layer, it is well-known that they overestimate the length scales within the viscous sublayer and are somewhat inaccurate at low Reynolds numbers. Following McDonald and Fish (ref. 12) the experimentally observed damping effect in the viscous sublayer is modeled by assuming intermittent turbulence within the sublayer leading to the relation

$$-\overline{u'v'} = \Gamma (-\overline{u'v'})_{\tau} = \Gamma (\ell \partial \bar{u} / \partial y)_{\tau}^2 = \left(\mathcal{D} \ell_{\tau} \frac{\partial \bar{u}}{\partial y} \right)^2 \quad (25)$$

In Eq. (25) Γ is the intermittency factor, \mathcal{D} the damping factor, and the subscript τ indicates the value with turbulent flow. Obviously, \mathcal{D} is equal to the square root of Γ . As in ref. 12, the present investigation assumes that the damping distributes normally about a mean height y^* ($y^* = y \sqrt{\tau / \rho / \nu}$) with a standard deviation σ leading to the equation

$$\mathcal{D} = P^{1/2} \{ (y^* - \bar{y}^*) / \sigma \} \quad (26)$$

where P is the normal probability function; \bar{y}^* is taken as 23, and σ as 8. A detailed discussion of the sublayer damping treatment is presented in ref. 12. In the present calculations the von Karman constant κ was taken to be 0.43.

In regard to the low Reynolds number effects, Coles (ref. 20) has observed and correlated the departure of the mean velocity profile of a flat plate turbulent boundary layer from the usual similarity laws known to hold at higher Reynolds numbers. Using Coles' correlation of the mean velocity profile in the low Reynolds number regime, McDonald (ref. 21) integrated the boundary layer equations of mean motion to obtain local distributions of turbulent shear stress and evaluated the local mixing length distributions from the assumed mean velocity distribution and the computed shear stress distributions. Based upon these calculations, a low Reynolds number correction for the dissipation length of the form

$$L = L_{\infty} \left[1 + \exp(-1.63 \ln R_{\theta} + 9.7) \right] \quad (27)$$

was derived where L_{∞}/δ is given by Eq. (23). In the calculations presented in the present report the dissipation length used was obtained by multiplying Eq. (27) by the sublayer damping factor, \mathcal{D} .

When numerical values of the structural coefficients a_n are specified, Eqs. (24), (26), and (27) are used to represent L and ℓ , and the pressure dilatation is either neglected or modeled, the turbulence kinetic energy equation, Eq. (19), becomes an ordinary differential equation with the dependent parameter $\ell_{\infty}(x)$ which is solved in conjunction with the boundary layer momentum and energy equations to predict the development of both the mean flow field and the turbulent shear stress.

In addition to including the turbulence kinetic energy equation in the set of equations governing the boundary layer development it is necessary to specify a model for turbulent heat flux contribution, $-\bar{\rho} C_p \overline{v' T'}$. As previously stated, in the present procedure, $\overline{v' T'}$ is specified by assuming a turbulent Prandtl number, Pr_T , which relates the velocity-temperature correlation, $\overline{v' T'}$, to the Reynolds stress, $\overline{u' v'}$, through Eq. (8). The turbulent Prandtl number distribution used in the present procedure varies with distance from the wall in the manner suggested by Meier and Rotta (ref. 22). At this juncture it should be pointed out that an alternative procedure can be used to determine $\overline{v' T'}$, based upon an easily derived conservation equation for either the quantity $\overline{T'^2}$ or the correlation, $\overline{v' T'}$, which is similar in form to the turbulence kinetic energy equation, Eq. (15). However, to solve this new conservation equation it is necessary to assume a universal structure relating quantities analogous to dissipation,

production, etc. While sufficient experimental data exists to allow valid modeling of the required terms for the turbulence kinetic energy equation, the existing data does not indicate how proper modeling could be carried out for the $\sqrt{T'}$ conservation equation. Thus, at least for the present, the approach based upon a turbulent Prandtl number appears preferable to an approach based upon the $\sqrt{T'}$ conservation equation.

Original transitional turbulence model. - The McDonald-Fish transitional turbulence model is based upon a solution of the turbulence kinetic energy equation with the structural coefficients modified from their fully-developed turbulence values. The following discussion of the model condenses the presentation in ref. 12. For fully-developed turbulent flows the structural coefficients Q_1 , Q_2 , and Q_3 are assumed constant and are set equal to 0.15, 0.50, and 0.20, respectively. Although it is probable that all coefficients vary in the transitional regime only the coefficient Q_1 contributes significantly to the energy balance when the boundary layer is far removed from separation, as shown by Bradshaw (ref. 19). Therefore, the transition model assumes Q_2 and Q_3 are equal to their fully-developed values and that only Q_1 need be modified. At this juncture it should be mentioned that in a recent unpublished study at UARL concerned with the prediction of transitional separation bubbles, Briley and McDonald have found it necessary to modify the values for Q_2 and Q_3 slightly, however, sample calculations indicate that the calculations presented in the present report are quite insensitive to the assumed values of Q_2 and Q_3 .

On the basis of current knowledge, it is expected that the structural coefficient Q_1 would depend both upon the applied strain, $\partial \bar{U} / \partial y$ and the ratio of the total effective viscosity to the kinematic viscosity. In regard to the first of these effects, the applied strain, both the experiments of Rose (ref. 23) and the analysis of Shamroth and Elrod (ref. 24) indicate that for large ratios of effective to kinematic viscosity the adjustment of Q_1 from an initial value to its fully-strained value occurs in a few boundary layer thicknesses. Transition to turbulence, on the other hand, typically takes place over a distance of many boundary layer thicknesses and, thus, if the effects of viscosity are ignored, the adjustment of Q_1 to its fully-developed value under the influence of mean strain can be considered instantaneous in comparison with the time scale of transition. Initial attempts to predict transitional flows, used a fully-strained value of $Q_1 = 0.15$. However, it soon became apparent that accurate predictions of transition required a much lower value for Q_1 and, consequently, McDonald and Fish (ref. 12) assumed the departure of Q_1 from its fully-developed value was due solely to the effect of viscosity. The relationship between Q_1 and viscosity was quantified by introducing a turbulent

Reynolds number, R_T . In defining R_T the velocity scale is taken as $(-\overline{u'v'})^{1/2}$ and the length scale is taken as the conventional mixing length, l , so that

$$R_T = \frac{(-\overline{u'v'})^{1/2} l}{\nu} \quad (28)$$

Noting that

$$(-\overline{u'v'}) = l^2 \left(\frac{\partial \bar{u}}{\partial y} \right)^2 = \nu_T \frac{\partial \bar{u}}{\partial y} \quad (29)$$

the turbulence Reynolds number becomes

$$R_T = \frac{\nu_T}{\nu} \quad (30)$$

To be consistent with the integral turbulence kinetic energy equation, Eq. (19), a layer-averaged turbulence Reynolds number, \bar{R}_T , is introduced as

$$\bar{R}_T = \frac{1}{\delta} \int_0^\delta \nu_T dy / \frac{1}{\delta_s} \int_0^{\delta_s} \nu dy \quad (31)$$

where δ_s , the sublayer thickness, is defined as the location at which the laminar stress has fallen to four percent of the total stress (the four percent definition gave a sublayer mean temperature in very good agreement with the so-called Eckert reference temperature).

The McDonald-Fish model assumes that the turbulence Reynolds number, \bar{R}_T , is the sole variable influencing the development of q_1 and a relationship between q_1 and \bar{R}_T is obtained by considering the development of an incompressible constant pressure flat plate equilibrium turbulent boundary layer. It should be noted that under the assumption that q_1 is solely dependent upon \bar{R}_T it is only necessary to derive a relation for one set of flow conditions to obtain a universally valid relationship. Based upon experimental observation, it is readily

ascertained that for the incompressible constant pressure equilibrium turbulent boundary layer, ϕ_3 , E , and $\partial \phi_1 / \partial x$ are negligible which leads to the reduced turbulence kinetic energy equation

$$\frac{d \ln a_1}{d R_\theta} = \frac{d \ln \delta}{d R_\theta} - \frac{4 a_1 \phi_2 \theta}{R_\theta C_f \phi_1 \delta} \quad (32)$$

In Eq. (32), C_f is the skin friction coefficient and the independent variable has been changed from streamwise distance, x , to momentum thickness Reynolds number, R_θ , using the momentum integral equation. Equation (32) has the general form of a Bernoulli equation

$$\frac{d \ln a}{d R_\theta} = f(R_\theta) + a_1 g(R_\theta) \quad (33)$$

which has the general solution

$$a_1 = (\exp \int f d R_\theta) / (C - \int g \exp \int f d R_\theta d R_\theta) \quad (34)$$

When the mutual dependence between \bar{R}_T , f , g , and R_θ is determined for the flat plate equilibrium boundary layer, Eq. (34) provides the required general relationship between a_1 and \bar{R}_T . The quantities f and g are evaluated by first noting that for the flat plate equilibrium boundary layer θ/δ varies very slowly with R_θ . Neglecting this variation leads to the result

$$f = \frac{1}{R_\theta} \quad (35)$$

The quantity g which is equal to the factor $-4 \phi_2 \theta / (C_f \phi_1 \delta)$ is evaluated numerically by integrating the profiles of Maise and McDonald (ref. 25). Over a wide range of Reynolds numbers the grouping is found to be sensibly constant with a value approximately 6.66. Thus, Eq. (34) becomes

$$\alpha_1 = \alpha_0 (R_\theta / R_{\theta_0}) / [1 + 6.666 \alpha_0 (R_\theta / R_{\theta_0} - 1)] \quad (36)$$

where the arbitrary constant α_0 is the value of α_1 when R_θ is equal to R_{θ_0} . It should be pointed out that at large values of R_θ / R_{θ_0} , α_1 asymptotes to the fully-developed value of 0.15. The independent variable of Eqs. (36) and (27) is changed from R_θ to \bar{R}_τ by using the profiles of Maise and McDonald (ref. 25) which integrate to give

$$R_\theta = 68.1 \bar{R}_\tau + 614.3 \quad \bar{R}_\tau > 40 \quad (37)$$

At low Reynolds numbers good results are obtained using the equation

$$R_\theta = 100 \bar{R}_\tau^{0.22} \quad \bar{R}_\tau \leq 1 \quad (38)$$

In the intermediate range $1 < \bar{R}_\tau < 40$, the two distributions, Eqs. (37) and (38), are joined by a cubic constructed to match the value and slope at the join points. Finally, the constant of integration, α_0 , is determined on the basis of comparison between experiment and theory. Best agreement between theory and experiment for low Mach number, adiabatic wall boundary layers is obtained by setting α_0 equal to 0.0115 when \bar{R}_τ is equal to unity. Then, from Eq. (38), $R_{\theta_0} = 100$.

Thus, in summary, the original transitional turbulence model is based upon three assumptions:

1. The development of the transitional boundary layer Reynolds stress is given by the turbulence kinetic energy equation.
2. The structural relations required to integrate the turbulence kinetic energy equation are identical in the fully-developed turbulent and transitional cases with one exception, that exception being the coefficient α_1 .
3. The structural coefficient α_1 is a universal function of the turbulence Reynolds number, \bar{R}_τ . The functional relationship is obtained from consideration of the incompressible flat plate equilibrium boundary layer.

Modified transitional turbulence model. - McDonald and Fish (ref. 12) demonstrated the ability of the original transitional turbulence model to predict transitional boundary layer behavior. They showed that the model accurately predicts the effect of free-stream turbulence upon near adiabatic wall boundary layers as well as the length of the transition region as a function of transition Reynolds number in both subsonic and moderately supersonic flows. In addition, the theory accurately predicts mean velocity profiles, integral thicknesses, Stanton number, and skin friction coefficients for a wide variety of transitional boundary layers. Details of all these comparisons are documented in ref. 12. In the present investigation the transitional turbulence model was used primarily in its original form, however, in the course of the investigation it became obvious that the original model did not properly predict the effect of wall temperature on boundary layer transition location. Although some controversy exists as to the effect of wall temperature on transition location, discussed in detail in the subsequent section, the general opinion is that increasing the wall temperature destabilizes the boundary layer. The data of Zysina-Molozhen and Kuznetsova (ref. 15) showing the effect of wall temperature upon transition location for a constant free-stream turbulence level in incompressible flow are presented in Fig. 1. As can be seen in Fig. 1, the data indicate increasing wall temperature destabilizes the boundary layer. In its original form the McDonald-Fish theory predicted heating to stabilize and cooling to destabilize the boundary layer, a prediction obviously in variance with the data and arising solely from the variation of viscosity with temperature. The theory was revised so that AB, the value of $2 \{u'v'\} / q^2$ at $\bar{R}_T = 1$, is a function of the wall-to-free-stream static temperature ratio, T_w/T_e . The functional relationship was chosen so that for incompressible flow the theory would agree with the data of Zysina-Molozhen and Kuznetsova in the range $0.5 < T_w/T_e < 2.8$. For $T_w/T_e > 2.8$ the transition Reynolds number was assumed to be independent of wall temperature ratio. The variation of AB with T_w/T_e required to allow the theory to predict the foregoing effect of wall temperature upon transition Reynolds number for a fixed disturbance level is shown in Fig. 2. It is, of course, quite reasonable to hypothesize that at a given Reynolds number the temperature gradient effects arising from wall heating would increase the amount of Reynolds stress created by turbulent intensity. Unfortunately, the extent of such an augmentation cannot presently be calculated and recourse must be made to empiricism.

COMPARISON WITH EXPERIMENT

Initiation of Transition

Primarily this investigation proposes to assess the applicability of the McDonald-Fish transitional turbulence model in the low hypersonic Mach number regime. Necessarily, for this purpose theoretical predictions of transitional boundary layer behavior must be compared with experimental data. Although a moderate amount of data exists for hypersonic transitional boundary layers, much of this data is contradictory, particularly as to the effect of flow variables such as Mach number, wall heating, etc. upon transition location. An example of the difficulty encountered in obtaining hypersonic transition data is demonstrated by the work of Stalmach, Bertin, Pope, and McCloskey (ref. 26). In Run 11, Condition 4 of ref. 26, Stalmach, et al., investigate transition on a 12 deg cone at an edge Mach number of 7. Transition was determined from heat transfer measurements taken along two rays of the cone surface. In these apparently carefully controlled experiments with no evidence for significant asymmetry in the flow, transition location on the two rays differed by approximately 15 percent. Since the two rays would have identical conditions for the purpose of making a theoretical prediction of boundary layer development, the 15 percent discrepancy in the transition Reynolds number gives an estimate of how closely theory and data can be expected to agree.

An important function of any transition theory is the prediction of transition location with various free-stream disturbances. In its original form, the McDonald-Fish transitional boundary layer theory successfully predicted the transition location as a function of free-stream turbulence for low-speed flows (ref. 12). The extension of this capability to moderately hypersonic flows was desired. In the present report transition is assumed to begin at that station where on a log-log plot straight line approximations to the Stanton number-Reynolds number curves in the laminar and transitional regimes intersect.

An immediate problem arises since the theory requires a free-stream turbulence intensity level as input and the (NASA) data documents a fluctuating pressure level. For the purpose of this investigation, the free-stream disturbance was assumed to be a plane wave propagating at a Mach number relative to the free stream. For such a disturbance the unsteady Bernoulli equation leads to a relation between fluctuating velocity and fluctuating pressure (e.g., ref. 27) of the form

$$\left| \frac{u'}{u_e} \right| = \frac{K}{\gamma M_e M_r} \left| \frac{p'}{p_e} \right| \quad (39)$$

where, as discussed by Laufer (ref. 27), K^{-1} may be thought of as the integral of a space-time correlation function. The relative Mach number, M_r , is assumed to be the function of M_∞ given by Laufer (ref. 27). If we further assume that the disturbance is an acoustic wave, v' and u' are related through the equation

$$|v'| = |u'| \sqrt{M_r^2 - 1} \quad (40)$$

The turbulence kinetic energy is then approximated by

$$\overline{q^2} = \overline{u'^2} + \overline{v'^2} + \overline{w'^2} \approx \frac{10}{7} (\overline{u'^2} + \overline{v'^2}) \quad (41)$$

Using the plane wave to model the disturbance, knowing the tunnel Mach number, M_∞ , and the boundary layer edge Mach number, M_e , the quoted free-stream fluctuating pressure, p'/p_e , easily converts to an equivalent turbulence kinetic energy velocity fluctuation u'/u_e which is used as input to the transitional boundary layer prediction procedure. Note that at this point it is also being assumed that the net acoustic energy absorbed by the boundary layer $\overline{p'v'} + (\rho v)' \overline{q^2}/2$ in the source term (Eq. (17)) is negligible in comparison with free-stream turbulence intensity entrained by the boundary layer and thus the source term E of Eq. (17) is assumed to be given by

$$E = \left[\frac{1}{2} \overline{q^2} \left(\bar{\rho} \bar{u} \frac{\partial \delta}{\partial x} - \bar{\rho} \bar{v} \right) \right]_e \quad (42)$$

Predictions obtained from the transitional boundary layer theory using both the original and modified transitional turbulence models are presented in Fig. 3 and compared to the data of Stainback (ref. 28). The original theory accurately predicts the variation of transition

Reynolds number with fluctuating pressure, however, this agreement requires a different value of K for the Mach 6 and Mach 8 tunnels.

The Mach 6 tunnel tests and the Mach 8 tunnel test were run for different values of wall temperature ratio. Since the original theory incorrectly predicts the effect of wall cooling on transition location, the calculations for initiation of transition were repeated using the modified theory. The comparison in Fig. 3 shows that the modified theory compares favorably with data when the same value of K is used for each tunnel. The single value of K for all three tunnels obtained with the modified theory represents a significant improvement over the results obtained with the original theory since it strongly supports the hypothesized relation between free-stream turbulence and the measured fluctuating pressure.

Rather than use free-stream turbulence intensity to trigger transition, it is possible to trigger transition by assuming a percentage of incident acoustic energy is absorbed directly by setting \bar{q}^2 at the outer edge of the boundary layer equal to zero and setting $(\bar{P}'V')$ equal to a nonzero value in the source term (see Eq. (17)). For an incoming acoustic wave, $P'v'$ is negative with respect to the boundary layer coordinate system and its magnitude can be estimated in terms of P'/P_e from Eqs. (39) and (40). The estimate was carried out assuming $K \approx 1$ and $\bar{P}'V'$ to be equal to $|P'| |v'|$ (i.e., the correlation coefficient $\bar{P}'V'/|P'| |v'| = 1$). If no energy were lost as the wave passed through the boundary layer, the wave would be reflected with undiminished strength and the contribution of the reflected wave at the edge of the boundary layer would be $-\bar{P}'V'$; thus, no net $\bar{P}'V'$ would result. However, the loss of some energy to the boundary layer could trigger transition. With this in mind, a study was initiated to determine what percent acoustic energy absorption, i.e., percent of $\bar{P}'V'$ absorption, would trigger transition. For the purpose of this qualitative investigation the quantity, $(\rho v)'q^2/2$, which is at most equal to and most likely less than $\bar{P}'V'$, is neglected and the source term, E , of Eq. (17) becomes

$$E = \left[-\bar{P}'V' \right]_e \quad (43)$$

The results of this study are presented in Fig. 4, where the theoretical predictions are compared to the experimental data of Stainback (ref. 29). As can be seen, the theory only requires a small amount of absorption to trigger transition at the streamwise station where transition occurs experimentally (a finding in agreement with the generally accepted

assumption that only a small amount of acoustic energy is lost as the wave passes through the boundary layer and reflects from the wall). Thus, it appears that if the amount of acoustic energy absorbed could be predicted from an independent analysis, the McDonald-Fish transition procedure contains a mechanism for predicting transition due solely to absorption of acoustic energy. Needless to say, no transition theory by itself can indicate whether hypersonic transition is triggered by free-stream turbulence or absorbed acoustic energy or some combination of the two. However, used in conjunction with experimentally measured input, the theory could indicate which of the two mechanisms is most likely to trigger transition.

Effect of free-stream Mach number. - The comparisons between theory and experiment presented in Figs. 3 and 4 were carried out at a constant edge Mach number, $M_e = 5$. An important question is, how is the transition location affected as the edge Mach number varies. To determine the effect of Mach number variation on transition location it would be necessary to run a series of experiments in which only the edge Mach number varied and all other quantities, particularly the free-stream disturbance and the ratio of wall-to-free-stream total temperature, were held constant. Such experiments have been carried out by several investigators in the range $0 < M_e < 4$ and the data is presented by Zysina-Molozhen and Kuznetsova in ref. 15. According to the data of ref. 15, the transition Reynolds number increases with edge Mach number in the entire range of Mach numbers considered. A second set of experiments determining transition location as a function of fluctuating pressure level for various Mach numbers has been reported by Stainback, Fischer, and Wagner (ref. 29). Based upon this data and that of Pate and Schueler (ref. 2), Stainback, Fischer, and Wagner conclude that Mach number has a strong effect on transition location in the range $5 < M_e < 14$. Furthermore, the data indicates a continuously stabilizing effect of increasing Mach number from $M_e = 5$ to $M_e = 16$ at a constant value of fluctuating pressure ratio P'/P_e . The continuously stabilizing effect of increasing Mach number upon transition even for $M_e < 3.5$ reported in ref. 15 is in contradiction with certain compilations of wind tunnel data which show that increasing the Mach number has a stabilizing effect for $M_e > 3.5$, but a destabilizing effect in the range $1.0 < M_e < 3.5$ (e.g., ref. 30). However, no reason exists to assume the data used in such compilations were all taken at the same disturbance level. In this regard, Morkovin (ref. 30) points out that free-flight cone data, which might be expected to have a smaller variation of disturbance intensity with Mach number than tunnel data, shows a continuously stabilizing effect of increasing Mach number even in the range $1.0 < M_e < 3.5$.

A somewhat different point of view as to the effect of edge Mach number on transition location has been expressed by Pate and Scheuler (ref. 2). Pate and Scheuler assume that the dominant effect on transition in supersonic wind tunnel experiments is the energy radiated from the tunnel wall boundary layers and not the Mach number per se. Following this assumption, Pate and Scheuler correlated transition location for a wide range of Mach numbers, $3 < M_e < 8$, with the wall boundary layer parameters and tunnel size without any explicit Mach number dependence. While the Pate-Scheuler correlation is quite useful in comparing transition experiments made in different facilities, it does not predict how a transitional boundary layer behaves in free flight, which is a problem of great interest. Furthermore, the Pate-Scheuler correlation is not in contradiction with a Mach number dependence of transition since disturbances emanating from the tunnel wall boundary layer vary with the free-stream Mach number.

With the above consideration in mind, a series of numerical calculations were run using the McDonald-Fish transitional boundary layer theory to predict the effect of free-stream Mach number on transition location at a given disturbance level, $u'/u_e = 0.03$. The variations of skin friction coefficient through the transitional regime as predicted using both the original and modified transitional turbulence models for a range of Mach numbers at a free-stream turbulence level, u'/u_e , equal to 0.03 and an adiabatic wall are presented in Fig. 5. Both the original and modified theories predict that increasing the Mach number stabilizes the boundary layer, although the modified theory predicts a considerably weaker stabilizing effect than that predicted by the original theory. The predicted stabilizing effect of Mach number for a given free-stream disturbance level and wall temperature ratio is believed to be in agreement with experiment, although, as mentioned previously, some controversy exists on interpretation of the various experimental data. It should be noted that in Fig. 5 the predicted fully-turbulent value of skin friction shows agreement with the turbulent prediction of van Driest (ref. 31). The variation of transition location predicted by both forms of the present prediction theory is compared with the data correlation over a range of free-stream disturbances compiled by Zysina-Molozhen and Kuznetsova (ref. 15) in Fig. 6. The theoretical calculations presented in Fig. 6 were carried out for $u'/u_e = 0.03$. The modified theory is in good agreement with experiment, particularly in the low hypersonic Mach number regime where it represents a significant improvement over the original theory.

Effect of wall temperature. - As previously mentioned, the wall temperature ratio, T_w/T_{ow} , may represent another important parameter which influences transition location. Experimental evidence on the

effect of varying wall temperature is more contradictory than that of varying Mach number. For example, Zysina-Molozhen and Kuznetsova (ref. 15), van Driest and Boison (ref. 32), and Cary (ref. 33) all observed cooling to stabilize the boundary layer on smooth walls. On the other hand, Sanator, DeCarlo, and Torillo (ref. 34) observed no effect of wall cooling and Richards and Stollery (ref. 35), and Sheetz (ref. 36) observed, under certain limited conditions, a destabilizing effect of wall cooling.

As in the case of the previously discussed effect of Mach number upon transition location, some of the contradictory evidence regarding the effect of wall cooling is due to variation of the free-stream disturbance level as the wall temperature ratio changed. However, in the case of wall cooling a new phenomenon may arise. As pointed out by van Driest and Boison (ref. 32), among others, as the wall temperature is lowered, the boundary layer thickness decreases making the ratio of the effective roughness height to the boundary layer thickness progressively larger. As cooling continues, a wall temperature may be reached at which the stabilizing effect of cooling is offset by the destabilizing effects of roughness. In evaluating the various wall cooling data, it should again be emphasized that the data discussed by Zysina-Molozhen and Kuznetsova (ref. 15), which includes data from the supersonic experiments of Higgins and Pappas (ref. 37), specified the free-stream turbulence as wall temperature was varied and it was this data which was used to evaluate the modified transitional turbulence model.

Several sets of calculations were performed using the McDonald-Fish transitional boundary layer theory to predict the effect of wall cooling on transition location. As shown in Fig. 7, the original theory predicts a destabilizing effect of wall cooling which is contradictory to the majority of smooth wall experimental evidence, however, the modified theory predicts a stabilizing effect of wall cooling. In regard to the predicted effect of wall cooling, it should be recalled that the modified transitional turbulence model was developed by matching theory and experiment in the incompressible regime and, thus, the predicted stabilizing effect of wall cooling at $M_e = 4.8$ is not an automatic consequence of the model assumptions.

Boundary Layer Behavior Through Transition

Prediction of Stanton number. - A major motivation in developing a procedure to predict the behavior of transitional boundary layers is the large heat flux which occurs at the end of the transitional regime. This large heat flux may lead to peak values of wall temperature which must be predicted accurately to insure structural integrity. Comparisons between predictions of transitional heat transfer from the McDonald-Fish theory and the experimental data of Stainback (ref. 29) are shown in Fig. 8. In the case of both the 20 inch tunnel and the Mach 8 tunnel data the transition length scale is predicted quite accurately. In addition, although not shown, the theoretical predictions of transition length are in good agreement with the semiempirical criteria used by Harris (ref. 4) in successfully predicting a wide variety of transitional boundary layers. The predictions of fully-turbulent Stanton number for the 20 inch hypersonic tunnel presented in Fig. 8 are approximately ten to twenty percent below the measured values; however, in the laminar regime the theoretical predictions are in excellent agreement with the theory of Cohen (ref. 38), whereas the data is again fifteen percent higher. Since there is no apparent reason for the experimental heat transfer to be higher than the predicted heat transfer upstream of transition, it was concluded that the 20 inch tunnel experimental data was uniformly in error. The fully-turbulent Stanton number predictions for the Mach 8 tunnel flow conditions are in good agreement with data. It should be noted that the results presented in Fig. 8 differ from those of ref. 29. The theoretical predictions presented in ref. 29 were preliminary predictions obtained with a theory having a slightly different sublayer model than that used in the present calculations. A second set of Stanton number predictions carried out for the data of Holloway and Sterrett (ref. 39) are presented in Fig. 9. For this comparison predictions of both the length of the transition region and the Stanton number distribution itself are in good agreement with data. In contrast to the case of the Stainback data, although a discrepancy between theory and experiment does appear in the peak value of Stanton number, the predicted maximum Stanton number in this instance exceeds the experimental value by approximately 15 percent. While no definite conclusion can be reached concerning the accuracy of the results in the fully-turbulent regime, the theoretical predictions are in good agreement with the flat plate analysis of van Driest (ref. 31); whereas the experimentally observed values are lower. For the above predictions of transitional Stanton numbers the input free-stream turbulence level was chosen to give agreement between the theoretically predicted and experimentally observed transition locations. This was also done in obtaining the predicted transitional velocity profiles subsequently presented.

Prediction of mean velocity profiles. - A stringent test for assessing the ability of a boundary layer calculation procedure to predict transitional behavior is the comparison between predicted and experimental mean velocity profiles. For this reason three comparisons between measured and predicted velocity profiles were made during this investigation. The first of these compares the theoretical predictions of the McDonald-Fish transitional boundary layer theory with the experimental data of O'Donnell (ref. 40). For this comparison, as for all other comparisons where no free-stream turbulence was quoted, a turbulence level of u'/u_e was chosen which initiated transition at the experimentally observed streamwise location.

A comparison between the theoretically predicted and experimentally measured velocity profiles is presented in Fig. 10. Some minor discrepancies between theory and experiment exist in the profile wall region where measurement difficulties would be expected, however, elsewhere the predictions are in excellent agreement with the laminar theory presented by O'Donnell (ref. 40) and the discrepancy in the transitional regime does not exceed that in the laminar regime. Therefore, the theoretical prediction should be regarded as good. A comparison between theoretically predicted and experimentally measured momentum thickness is presented in Fig. 11 which again shows good agreement between theory and experiment.

A second set of calculations was carried out to compare the McDonald-Fish theory with the Michel and Schmitt profile data (ref. 41) presented in Fig. 12. Both the fully-laminar and fully-turbulent predicted profiles are in good agreement with data, as is the length of transition region, however, within the transitional regime itself the agreement is not very good. The data was measured on a cylindrical rod with a radius only four times the boundary layer thickness. No account of the finite value ratio of the rod radius to boundary layer thickness was taken in the calculation and this may explain some of the discrepancy. A slight adverse pressure gradient in the experiment represents a second possible source of error. The experimentally determined edge Mach number distribution showed considerable scatter between $M_e = 6.65$ and $M_e = 6.55$ and for the purpose of the calculation the edge Mach number was assumed constant at a value of 6.6. Comparison of integral thicknesses and Stanton number are presented in Figs. 13 and 14. As can be seen in Fig. 14, the measured Stanton numbers do not agree with either the McDonald-Fish theory or the theory of Cohen in the laminar regime, thus making the transitional comparisons doubtful.

The final comparison between theoretically predicted and experimentally measured profiles was made for the NASA Langley Research Center data of Fischer and Maddalon (ref. 42), which contains both mean velocity and density profiles. Comparisons between the theory and experiment for the velocity profiles is presented in Fig. 15 and for the density profiles in Fig. 16. Both the predicted length of the transition region and the velocity profiles are in reasonably good agreement with experiment. Although the density profiles are not as well predicted as the mean velocity profiles, they are still quite acceptable, particularly considering the large density gradients through the midportion of the boundary layer. General agreement is shown between measured and predicted displacement thickness presented in Fig. 17. In summary, it seems that considering the uncertainties in the measured data, the comparisons between the predicted and measured mean velocity profiles are quite good.

The Role of Fluctuating Pressure

Two major assumptions which are made in deriving the turbulence kinetic energy equation should be reexamined in the hypersonic flow regime. These concern the direct roles of fluctuating density and fluctuating pressure. As shown in APPENDIX B, the most likely direct contribution of fluctuating density to the turbulence kinetic energy balance occurs in the turbulence production mechanism where the terms $\bar{v}\rho'u'\partial\bar{u}/\partial y$ and $\bar{\rho}'u'v'\partial\bar{u}/\partial y$ are neglected in comparison to $\bar{\rho}u'v'\partial\bar{u}/\partial y$. The ratios of the neglected to the included terms are given by

$$\frac{\bar{v}}{\bar{\rho}} \frac{\bar{\rho}'u'}{\bar{u}'v'} \approx \frac{|\rho'|/\bar{\rho}}{|v'|/\bar{v}}, \quad \frac{\bar{\rho}'u'v'}{\bar{\rho}u'v'} \lesssim \left| \frac{\rho'}{\bar{\rho}} \right| \quad (44)$$

In the boundary layers investigated in the present investigation it appears likely that these ratios remain small and, thus, it does not appear that in the low hypersonic Mach number regime fluctuating density makes a major contribution to the turbulence energy balance.

The role of fluctuating pressure terms, however, is not as obvious. As previously discussed, pressure fluctuations may play a major role in the transition process by acting as a source term in the turbulence kinetic energy equation. The calculations presented in Fig. 4, show that only approximately 0.3 percent of the incident acoustic energy need be absorbed by the boundary layer in order to trigger transition at the observed location in absence of any free-stream turbulence kinetic energy, q^2 . A second mechanism through which

pressure fluctuations may influence transition is represented by the pressure dilatation term $P' \partial u'_i / \partial x_i$. Although this term is usually neglected in forming the turbulence energy balance, there is no reason to expect it to be insignificant in high Mach number flows. An estimate of its magnitude is obtained from the continuity equation in the following manner. When divided into mean and fluctuating parts the mean flow continuity equation is written as

$$\begin{aligned} \frac{\partial}{\partial t} (\bar{\rho} + \rho') + \frac{\partial}{\partial x_i} (\bar{\rho} + \rho') (\bar{u}_i + u'_i) &= \frac{\partial \bar{\rho}}{\partial t} + \frac{\partial \rho'}{\partial t} \\ &+ \frac{\partial \bar{\rho} \bar{u}_i}{\partial x_i} + \frac{\partial \rho' \bar{u}_i}{\partial x_i} + \frac{\partial \bar{\rho} u'_i}{\partial x_i} + \frac{\partial \rho' u'_i}{\partial x_i} = 0 \end{aligned} \quad (45)$$

Averaging Eq. (45) yields

$$\frac{\partial \bar{\rho}}{\partial t} + \frac{\partial \bar{\rho} \bar{u}_i + \overline{\rho' u'_i}}{\partial x_i} = 0 \quad (46)$$

which when subtracted from Eq. (45) leads to the result

$$\frac{\partial \rho'}{\partial t} + \frac{\partial \rho' \bar{u}_i}{\partial x_i} + \frac{\partial \bar{\rho} u'_i}{\partial x_i} + \frac{\partial \rho' u'_i - \overline{\rho' u'_i}}{\partial x_i} = 0 \quad (47)$$

or,

$$\frac{\partial \rho'}{\partial t} + \bar{u}_i \frac{\partial \rho'}{\partial x_i} + \rho' \frac{\partial \bar{u}_i}{\partial x_i} + u'_i \frac{\partial \bar{\rho}}{\partial x_i} + \frac{\partial}{\partial x_i} (\rho' u'_i - \overline{\rho' u'_i}) = -\bar{\rho} \frac{\partial u'_i}{\partial x_i} \quad (48)$$

As pointed out by Bradshaw and Ferris (ref. 8), Taylor's hypothesis leads to the conclusion

$$\frac{\partial \rho'}{\partial t} + \bar{u}_i \frac{\partial \rho'}{\partial x_i} = 0 \quad (49)$$

and, therefore,

$$\overline{P' \frac{\partial u'_i}{\partial x_i}} = - \frac{\overline{P' \rho'}}{\bar{\rho}} \frac{\partial \bar{u}_i}{\partial x_i} - \frac{\overline{P' u'_i}}{\bar{\rho}} \frac{\partial \bar{\rho}}{\partial x_i} + \overline{P' \frac{\partial \rho' u'_i}{\partial x_i}} \quad (50)$$

In view of the recent data of Owen and Horstman (ref. 43), Taylor's hypothesis must be used with caution in the transitional regime, however, the hypothesis is still good enough for the present order of magnitude arguments to be valid. When third order correlations and the mean flow dilatation is assumed small and the boundary layer approximations are made, the final expression for the pressure dilatation term becomes

$$\overline{P' \frac{\partial u_i}{\partial x_i}} = - \frac{\overline{P' v'}}{\bar{\rho}} \frac{\partial \bar{\rho}}{\partial y} \quad (51)$$

If a suitable model for $\overline{P' v'}$ is hypothesized, the approximation to the pressure-dilatation term can be included in the turbulence kinetic energy equation.

In hypothesizing a model for the factor $\overline{P' v'}$ to be used in the present investigation to determine the contribution of the pressure-dilatation term in the turbulence kinetic energy equation, the assumption was made that the $\overline{P' v'}$ to be used should be that generated in the boundary layer rather than that which propagates in from the free stream and is absorbed by the boundary layer. Based upon the data obtained by Bradshaw (ref. 19) and Laufer (ref. 44), $\overline{P' v'}$ was assumed constant across the boundary layer. The assumption of constant $\overline{P' v'}$ with distance from the wall is obviously in error at the wall where $\overline{P' v'}$ must be zero, however, the data does indicate $\overline{P' v'}$ is constant in the outer region. The magnitude of $\overline{P' v'}$ was obtained by noting that Kistler and Chen (ref. 45) measured $|\overline{P'_w}|/\tau_w$ in fully-turbulent flow to be a function of edge Mach number, M_e . For transitional flow this relation was modified to

$$P' = \tau_w f(M_e) \frac{\int_0^\delta \nu_T dy}{\int_0^\delta \nu_T + \nu dy} \quad (52)$$

where ν is the kinematic viscosity, ν_T is the turbulent kinematic viscosity and $f(M_e)$ is obtained from the Kistler-Chen data.

The fluctuating velocity v' was estimated from

$$\overline{v'^2} = \frac{0.2}{8} \int_0^8 \overline{q^2} dy \quad (53)$$

which is known to overestimate the value of $\overline{v'^2}$ in transitional flows. Using these assumptions and assuming, furthermore, that $P'v'/|P'||v'| = 1.0$ the normalized pressure-dilatation term becomes

$$\frac{\overline{P'}}{\rho_e u_e^3} \frac{\partial u_i}{\partial x_i} = - \frac{|P'| |v'|}{\rho_e u_e^3} \frac{1}{\bar{\rho}} \frac{\partial \bar{\rho}}{\partial y} \quad (54)$$

where $|P'|$ and $|v'|$ are obtained from Eqs. (52) and (53), respectively. Since $P'v'$ is positive (ref. 19), the pressure-dilatation term acts as a turbulent sink. A comparison of calculations carried out, including and omitting the pressure-dilatation term, is presented in Fig. 18. The calculations presented in Fig. 18 were made assuming the turbulent source term, E , of Eq. (17) to be given by

$$E = \left[\frac{1}{2} \overline{q^2} (\bar{\rho} \bar{u} \frac{\partial \delta}{\partial x} - \overline{\rho v}) \right]_e \quad (55)$$

The magnitude of $\overline{q^2}$ was chosen by relating the fluctuating velocity to the measured fluctuating pressure through Eq. (39). It should be noted that Eq. (39) contains an empirical constant which was evaluated by comparing theoretical calculations which neglect pressure-dilatation effects with experimental data. Since the data presented in Fig. 18 was one of the sets of data used in evaluating the empirical constant, the theory neglecting pressure-dilatation effects shows better agreement with data than the theory including pressure-dilatation effects. However, the important conclusion to be drawn from Fig. 18 is that although it was given its maximum reasonable value, inclusion of the pressure-dilatation term made only a minor difference in transition location and no difference in the shape of the Stanton number-Reynolds number curve. Thus, at the present time in view of the uncertainty of the assumptions which must be made in modeling the pressure-dilatation

effect, little advantage accrues to the inclusion of the pressure-dilatation term in the turbulent energy balance for these conditions where $M_e = 5.0$ and $T_w/T_0 \approx 0.6$.

The Precursor Effect

Hot wire anemometer studies show that significant oscillations occur in the outer portion of the boundary layer far upstream of the transition location determined by wall instrumentation (refs. 29, 46 and 47). These oscillations, termed the 'precursor effect', are associated with the onset of transition, and initially appear in the vicinity of the critical layer and spread at an angle of approximately 0.5 deg relative to the wall. Thus it is expected that the precursor effect would first be noticed in hypersonic flow at approximately 150 boundary layer displacement thicknesses upstream of the streamwise station at which transition is recognized from heat transfer measurements. The McDonald-Fish theory in solving the turbulence kinetic energy equation in nominally laminar flow also predicts such a precursor effect. According to the theory a small amount of Reynolds stress first appears in the outer portion of the boundary layer far upstream of the station at which the wall properties depart from their laminar variation. The region of significant Reynolds stress spreads as the flow proceeds downstream and when this region approaches the wall, the wall properties such as Stanton number and skin friction differ from laminar. A plot of computed normalized stress profiles for conditions corresponding to those for Stainback's Mach 8 tunnel data (ref. 29) at several selected stations, presented in Fig. 19, shows that at 200 displacement thicknesses upstream of the transition location a small amount of kinematic Reynolds stress appears in the outer portion of the boundary layer. The transition location, x_T , was again determined by the intersection of straight line fairing in a log-log plot of Stanton number versus Reynolds number. As the flow proceeds downstream, the Reynolds stress increases in magnitude and transverse extent. Significantly the predicted transverse location at which the precursor effect first appears is in the outer portion of the layer in qualitative agreement with experimental data. Also, the predicted spreading angle for the particular case considered is approximately 0.3 deg, also in qualitative agreement with experimental data (ref. 47).

DISCUSSION

The problem of predicting the initiation of transition and the behavior of boundary layers through the transitional regime is one of the most difficult problems encountered in boundary layer theory. However, the contradictory experimental evidence as to the effect of Mach number (e.g., refs. 2, 15, and 30) or wall cooling (e.g., refs. 15, 30, and 32 through 36) clearly indicate the need for developing a transition prediction procedure based upon as low a degree of empiricism as possible. In addition to the effect of Mach number and wall cooling other phenomenon not considered in the present investigation such as streamwise pressure gradient, roughness (e.g., refs. 30, 39, and 48 through 50) and unit Reynolds number (e.g., refs. 2, 3, 29, 30, and 48) may also have important effect on transitional boundary layer behavior. Tunnel effects which further complicate the data assessment problem (refs. 2, 3, and 29) may make valid comparisons between data taken in different wind tunnels difficult and, more importantly, may make the correct application of wind tunnel data to free-flight conditions doubtful unless the wind tunnel data is obtained under stringent control.

With these considerations in mind, the advantages of a general transitional theory such as that described here are evident. In the present report, the theory has been examined in four respects: the ability to predict (1) the initiation of transition; (2) the effect of parametric variation upon transition; (3) heat transfer through transition; and (4) velocity and density profiles through transition. The calculations to ascertain if the procedure could predict transition location as a function of the free-stream disturbance level were based upon the free-stream disturbance as a vorticity fluctuation, i.e., free-stream turbulence intensity. At higher Mach numbers, $M_e > 2.5.$, in addition to the free-stream turbulence the disturbance field contains both a sound mode (refs. 2 and 3) and an entropy mode. Although the entropy mode is unlikely to be important except at very high Mach numbers, it is possible that the sound mode may be the principal transition trigger, particularly with small vorticity fluctuations. However, even a dominant acoustic mode does not preclude free-stream fluctuating velocity entrainment by the boundary layer as the source of transition, since the fluctuating velocity field associated with the acoustic field could be entrained by the boundary layer and cause transition in the same manner as free-stream turbulence intensity causes transition at low Mach numbers. The calculations presented in Fig. 3, which are based on this concept of an associated fluctuating velocity field, are encouraging since the same value of K gives good agreement

between theory and experiment for three tunnels. Obviously, the theory would have to be tested over a much wider range of experiments before any definite conclusions could be made.

An alternative and direct source for transition is the absorption of the incident acoustic energy by the boundary layer. At present no way exists to estimate accurately what fraction of the energy of the incident acoustic wave is absorbed by the boundary layer, although this fraction absorbed must be small. The McDonald-Fish transitional theory predicts that less than one percent of the acoustic energy; i.e., less than one percent of $\overline{P'v'}$, need be absorbed to trigger transition (see Fig. 4). However, until the development of an adequate theory to predict acoustic energy absorption by a boundary layer, it is impossible to judge the reasonableness of a one percent energy absorption. In regard to the ability of the McDonald-Fish theory to predict the effect of parametric variation upon transition, predictions made with the modified theory for the variation of transition location with Mach number agree with the data compiled by Zysina-Molozhen and Kuznetsova (ref. 15), as shown in Fig. 6. In addition, the modified theory correctly predicts the effects of wall cooling in the absence of roughness, Fig. 7, at high Mach numbers. In regard to the other parameters, calculations presented by McDonald and Fish (ref. 12) show the theory successfully applied in the presence of streamwise pressure gradients and wall roughness for low speed flow. Based upon the success of the present investigation, these trends could probably be predicted accurately in the low hypersonic Mach number regime. The ability to predict variation of transition location with changes in flow parameters from the fundamental conservation equations is one of the chief advantages of the McDonald-Fish transitional theory.

Predictions of the Stanton number distribution through transitional flow indicate the theory accurately predicts the length of the transitional region in the low hypersonic Mach number regimes. Predictions of the Stanton number distribution itself appear to be good. In the case of the Stainback data (ref. 29), as shown in Fig. 8, within limits of experimental scatter, the theory predicts both the length of transition and the Stanton number accurately.

The final test of the McDonald-Fish transitional theory is the ability to predict mean velocity profiles. Although the predictions shown in Fig. 12 were not in good agreement with the data of Michel and Schmitt (ref. 41), the predictions shown in Figs. 10, 15, and 16 agreed with the data of O'Donnell (ref. 40) and the NASA Langley data of Fischer and Maddalon (ref. 42). The velocity profiles were calculated using the original theory, but no significant changes in this

regard are expected from the modified theory. Thus, on balance it is concluded that the McDonald-Fish transitional theory can accurately predict: (1) the length of transition, (2) transitional heat transfer, (3) transitional velocity profiles, and (4) effect of Mach number, wall temperature, and free-stream disturbance level upon relative transition location. In addition, the results are encouraging as to the theory's ability to predict quantitatively the absolute transition Reynolds number corresponding to a specified set of conditions and the theory predicts a precursor effect in qualitative agreement with that experimentally observed.

CONCLUSIONS

1. The McDonald-Fish transitional boundary layer theory shows considerable promise for predicting the transition Reynolds number at a given free-stream disturbance level in the low hypersonic Mach number regime.

2. The theory accurately predicts the change in transition location caused by the free-stream Mach number, wall temperature ratio, and free-stream disturbance level.

3. The theory contains mechanisms for triggering transition by free-stream turbulence entrainment or from direct acoustic energy absorption.

4. The theory accurately predicts the variation of mean velocity profiles, Stanton numbers, and integral thicknesses through the transitional regime for low hypersonic Mach number boundary layers.

5. The direct effects of fluctuating pressure through the pressure-dilatation contribution to the turbulence energy balance do not significantly alter the transition Reynolds number for low hypersonic Mach number boundary layers.

6. The theory predicts turbulence production in the boundary layer far upstream of the place where it is first noticeable at the wall (the precursor effect) similar to effects noticed experimentally.

RECOMMENDATIONS FOR FUTURE WORK

Further development and assessment of theoretical approaches for predicting transitional boundary layers must rely heavily on experimental guidance. New information of the type not previously generally measured in the transitional boundary layer, such as the development of the Reynolds stresses and the precise makeup of disturbance modes is urgently required. Given the very close relationship observed at low speeds between the intensity of the disturbance and the transition location, it is very surprising to find transition studies at high speeds where not even the free-stream disturbance level is measured.

Insofar as the present transitional theory is concerned, should further improvement in the predictions be found necessary, three possible areas of improvement can be investigated. The first of these concerns the turbulence structural hypothesis assumed for the transitional boundary layer and here more refined turbulence relationships can obviously be examined. Secondly, if sufficient confidence can be established in a pressure-velocity diffusion relationship, then it may prove rewarding to replace the integral representation of the turbulence kinetic energy equation by a finite-difference solution to the actual local partial differential equation. However, it is felt that the use of an integral form of the turbulence kinetic energy equation at the present time avoids the difficulty of explicitly specifying this largely unknown pressure-velocity relationship at the same time as simplifying the computation. These considerations lead to what is felt to be a more rewarding third area of investigation; that is, of replacing the turbulence kinetic energy equation used in the present theory by the three component intensity equations and the Reynolds apparent shear stress equation, again all initially in integral form. A preliminary investigation of this four equation integral representation has shown encouraging results in fully-turbulent boundary layer flow.

APPENDIX A

The Calculation Procedure

The procedure used to solve the momentum and energy equations is a Hartree-Womersley calculation procedure similar to that described by Smith and Clutter (ref. 51). In the calculation procedure the differential equations are transformed to a form more convenient for computer solution by introducing new variables

$$\eta = y/\delta^+ \quad (A-1)$$

$$F' = 1 - \frac{\bar{\rho} \bar{u}}{\rho_e u_e} \quad (A-2)$$

$$G' = \frac{T_e^0 - \bar{T}^0}{T_e^0 - T_{REF}} \quad (A-3)$$

$$\beta = \rho_e / \rho \quad (A-4)$$

where the primes indicate differentiation with respect to η , T^0 is the stagnation temperature, T_{REF} is a specified constant reference temperature, and δ^+ is a length scale usually taken to be the displacement thickness. In certain flows, such as the boundary layer developing on the cold wall nozzle, the displacement thickness may become small or even negative and in these cases δ^+ is taken to be a linear combination of the displacement thickness and a constant reference length such that δ^+ remains positive.

The momentum equation, Eq. (9), and the energy equation, Eq. (10), are solved by first eliminating ρv through the continuity equation, Eq. (3), and replacing the variables T^0 , ρ , and u by G' , F , and β . The streamwise derivatives are then replaced by finite differences leading to equations of the form

$$A_3 F''' + A_2 F'' + A_1 F' + A_0 F = A_4 \quad (A-5)$$

$$B_3 G''' + B_2 G'' + B_1 G' = B_4 \quad (A-6)$$

where A_n and B_n are functions of F , G' and their derivatives. The equations are linearized by assuming values for F , G' and their derivatives based upon the solution at the previous streamwise stations and the resulting linear differential equations are solved by Gaussian elimination using the boundary conditions

$$F'(0) = 1 - \frac{\rho_w u_w}{\rho_e u_e} \quad (A-7)$$

$$F'(\delta) = 0 \quad (A-8)$$

$$G'(0) = \frac{T_e^0 - T_w}{T_e^0 - T_{REF}} \quad \text{OR} \cdot \quad G''(0) = 0 \quad (A-9)$$

$$G'(\delta_{TH}) = 0 \quad (A-10)$$

where δ_{TH} is the thickness of the thermal boundary layer. In the calculations presented in the present report, u_w was always taken as zero. Having obtained the solution of the linearized equations, the distributions of F and G' are compared to the distributions used to evaluate the nonlinear coefficients, A_n and B_n . If the old and new distributions agree to within a specified tolerance, the procedure moves to the next streamwise station. If the two do not agree, the procedure is repeated. In the case of turbulent flow, the coefficients A_n and B_n , also depend on the turbulent kinematic viscosity, ν_T , and a turbulence kinetic energy equation is included in the iteration loop.

APPENDIX B

The Turbulence Kinetic Energy Equation

The turbulence kinetic energy equation is derived from the Navier-Stokes equations by multiplying the i^{th} Navier-Stokes momentum equation by the i^{th} component of fluctuating velocity and averaging the results (ref. 8). If the three average equations are then summed the result is

$$\begin{aligned} & (\bar{\rho} \bar{u}_j + \bar{\rho}' u'_j) \frac{\partial \bar{q}^2/2}{\partial x_j} + (\bar{\rho} \bar{u}'_i u'_j + \bar{u}_j \bar{\rho}' u'_i + \bar{\rho}' u'_i u'_j) \frac{\partial \bar{u}_i}{\partial x_j} \\ & + \frac{\partial}{\partial x_j} (\bar{\rho}' u'_j + 1/2 \overline{(\rho u_j)' q^2} - \overline{\sigma'_{ij} u'_i}) + \overline{\sigma'_{ij} \frac{\partial u'_i}{\partial x_j}} - \overline{\rho' \frac{\partial u_i}{\partial x_j}} = 0 \end{aligned} \quad (\text{B-1})$$

where q^2 is the turbulence intensity defined by

$$q^2 = u'^2 + v'^2 + w'^2 \quad (\text{B-2})$$

and σ'_{ij} is the fluctuating viscous stress tensor given by

$$\sigma'_{ij} = \lambda \frac{\partial u'_k}{\partial x_k} \delta_{ij} + \mu \left(\frac{\partial u'_j}{\partial x_i} + \frac{\partial u'_i}{\partial x_j} \right) \quad (\text{B-3})$$

where λ is the second coefficient of viscosity and δ_{ij} is the Kronecker delta defined as

$$\begin{aligned} \delta_{ij} &= 0 \quad i \neq j \\ \delta_{ij} &= 1 \quad i = j \end{aligned} \quad (\text{B-4})$$

Since it is assumed that

$$\frac{|\rho'|}{\bar{\rho}} \ll 1 \quad (\text{B-5})$$

$$\frac{|u'|}{\bar{u}} \ll 1 \quad (\text{B-6})$$

the first term is approximated as

$$(\bar{\rho}\bar{u}_j + \overline{\rho'u'_j}) \frac{\partial q^2/2}{\partial x_j} \approx \bar{\rho}\bar{u} \frac{\partial \overline{q^2/2}}{\partial x} + (\bar{\rho}\bar{v} + \overline{\rho'v'}) \frac{\partial \overline{q^2/2}}{\partial y} \quad (\text{B-7})$$

Similarly the next set of terms is expanded as

$$\begin{aligned} & (\bar{\rho}\overline{u'_i u'_j} + \bar{u}_j \overline{\rho' u'_j} + \overline{\rho' u'_i u'_j}) \frac{\partial \bar{u}_i}{\partial x_j} = \\ & (\bar{\rho}\overline{u' u'} + \bar{u} \overline{\rho' u'} + \overline{\rho' u' u'}) \frac{\partial \bar{u}}{\partial x} + \\ & (\bar{\rho}\overline{u' v'} + \bar{v} \overline{\rho' u'} + \overline{\rho' u' v'}) \frac{\partial \bar{u}}{\partial y} + \\ & (\bar{\rho}\overline{v' u'} + \bar{u} \overline{\rho' v'} + \overline{\rho' v' u'}) \frac{\partial \bar{v}}{\partial x} + \\ & (\bar{\rho}\overline{v' v'} + \bar{v} \overline{\rho' v'} + \overline{\rho' v' v'}) \frac{\partial \bar{v}}{\partial y} \end{aligned} \quad (\text{B-8})$$

Since by the boundary layer approximations

$$\left| \frac{\partial(\overline{\quad})}{\partial y} \right| \gg \left| \frac{\partial(\overline{\quad})}{\partial x} \right| \quad (\text{B-9})$$

$$|\bar{u}| \gg |\bar{v}| \quad (\text{B-10})$$

Equation (B-8) becomes

$$\begin{aligned}
 & \left(\bar{\rho} \overline{u'_i u'_j} + \bar{u}_j \overline{\rho' u'_i} + \overline{\rho' u'_i u'_j} \right) \frac{\partial \bar{u}_i}{\partial x_j} \approx \bar{\rho} \overline{u' u'} \frac{\partial \bar{u}}{\partial x} \\
 & + \bar{u} \overline{\rho' u'} \frac{\partial \bar{u}}{\partial x} + \bar{\rho} \overline{u' v'} \frac{\partial \bar{u}}{\partial y} + \bar{v} \overline{\rho' u'} \frac{\partial \bar{u}}{\partial y} + \\
 & \overline{\rho' u' v'} \frac{\partial \bar{u}}{\partial y} + \bar{\rho} \overline{v' v'} \frac{\partial \bar{v}}{\partial y} + \bar{v} \overline{\rho' v'} \frac{\partial \bar{v}}{\partial y} + \overline{\rho' v' v'} \frac{\partial \bar{v}}{\partial y}
 \end{aligned} \tag{B-11}$$

From the boundary layer approximations

$$\frac{\partial \bar{u}}{\partial y} \gg \frac{\partial \bar{u}}{\partial x} \approx \frac{\partial \bar{v}}{\partial y} \tag{B-12}$$

and from experimental evidence

$$\bar{\rho} \overline{u' v'} \approx \bar{\rho} \overline{u' u'} \approx \bar{\rho} \overline{v' v'} \tag{B-13}$$

Although only a small number of measurements for $\rho'/\bar{\rho}$ exist in the low hypersonic Mach number regime, Harvey, Bushnell, and Beckwith (Ref. 52) have shown that in this regime the available evidence indicates

$$\frac{|\rho'|}{\bar{\rho}} \lesssim 0.2 \tag{B-14}$$

Eq. (B-14) is assumed valid for flow conditions considered in the present report. Thus,

$$\begin{aligned}
 & \left(\bar{\rho} \overline{u'_i u'_j} + \bar{u}_j \overline{\rho' u'_i} + \overline{\rho' u'_i u'_j} \right) \frac{\partial \bar{u}_i}{\partial x_j} \approx \bar{\rho} \overline{u' v'} \frac{\partial \bar{u}}{\partial y} \\
 & + \bar{\rho} \overline{u' u'} \frac{\partial \bar{u}}{\partial x} + \bar{\rho} \overline{v' v'} \frac{\partial \bar{v}}{\partial y} + \overline{\rho' u' v'} \frac{\partial \bar{u}}{\partial y} + \bar{v} \overline{\rho' u'} \frac{\partial \bar{u}}{\partial y}
 \end{aligned} \tag{B-15}$$

Although the second and third terms are usually small compared to the first, they are retained since they represent production by normal stresses in incompressible flow and may become important in the region of separation or transition. For subsonic and moderately supersonic flow in the absence of wall heating, order of magnitude arguments indicate the last two terms are small compared to the first term (ref. 8) and they are neglected in the present formulation. (In the case of high Mach number flows or flows with significant wall heat transfer, it may become important, if $|\rho'|/\bar{\rho} \approx |v'|/\bar{v}$.) With the above approximations, Eq. (B-11) becomes

$$\left(\bar{\rho} \overline{u_i' u_j'} + \bar{u}_j \overline{\rho' u_i'} + \overline{\rho' u_i' u_j'} \right) \frac{\partial \bar{u}_i}{\partial x_j} \approx$$

(B-16)

$$\bar{\rho} \overline{u' v'} \frac{\partial \bar{u}}{\partial y} + \bar{\rho} \overline{u' u'} \frac{\partial \bar{u}}{\partial x} + \bar{\rho} \overline{v' v'} \frac{\partial \bar{v}}{\partial y}$$

Following ref. 8 it is assumed that viscous diffusion is negligible. Thus the turbulence kinetic energy equation becomes

$$\bar{\rho} \bar{u} \frac{\partial \overline{q^2/2}}{\partial x} + \bar{\rho} \bar{v} \frac{\partial \overline{q^2/2}}{\partial y} + \bar{\rho} \overline{u' v'} \frac{\partial \bar{u}}{\partial y} + \bar{\rho} \overline{u' u'} \frac{\partial \bar{u}}{\partial x} +$$

(B-17)

$$\bar{\rho} \overline{v' v'} \frac{\partial \bar{v}}{\partial y} + \frac{\partial}{\partial y} \left(\overline{\rho' v'} + \overline{1/2 (\rho v)' q^2} \right) + \sigma'_{ij} \frac{\partial u'_i}{\partial x_j} - \overline{\rho' \frac{\partial u'_i}{\partial x_j}} = 0$$

Using the equation of continuity the turbulence kinetic energy equation is put in final form as

$$\begin{aligned} & \frac{\partial}{\partial x} \left(\frac{1}{2} \bar{\rho} \bar{u} \overline{q^2} \right) + \frac{\partial}{\partial y} \left(\frac{1}{2} \bar{\rho} \bar{v} \overline{q^2} \right) = - \overline{\rho u' v'} \frac{\partial \bar{u}}{\partial y} + \overline{\rho' \frac{\partial u'_i}{\partial x_i}} \\ & \text{advection (mean flow convection)} \qquad \text{production} \qquad \text{pressure-dilatation} \\ & - \frac{\partial}{\partial y} \left(\overline{\rho' v'} + \overline{1/2 (\rho v)' q^2} \right) - \bar{\rho} \epsilon - \bar{\rho} \left(\overline{u'^2 v'^2} \right) \frac{\partial \bar{u}}{\partial x} \\ & \text{diffusion} \qquad \text{dissipation} \qquad \text{normal stress term} \end{aligned}$$

(B-18)

where ϵ represents the sum of the turbulent dissipation terms. In obtaining Eq. (B-18) the normal stress term (which did not make a noticeable contribution to the turbulence kinetic energy balance for calculations presented in the present report) it was assumed that

$$\frac{\partial \bar{u}}{\partial x} + \frac{\partial \bar{v}}{\partial y} = 0 \quad (\text{B-19})$$

REFERENCES

1. Hairston, D. E.: Survey and Analysis of Current Boundary Layer Transition Prediction Techniques. Preprint No. 71-985, AIAA, October 1971.
2. Pate, S. R. and Schueler, C. J.: Radiated Aerodynamic Noise Effects on Boundary Layer Transition in Supersonic and Hypersonic Wind Tunnels. AIAA Journal, Vol. 7, No. 3, March 1969, pp. 450-457.
3. Pate, S. R.: Measurements and Correlations of Transition Reynolds Numbers on Sharp Slender Cones at High Speeds. AIAA Journal, Vol. 9, No. 6, June 1971, pp. 1082-1090.
4. Harris, J. E.: Numerical Solution of the Equations for Compressible Laminar, Transitional and Turbulent Boundary Layers and Comparison with Experimental Data. NASA TR R-369, August 1971.
5. Dhawan, S. and Narashima, R.: Some Properties of Boundary Layer Flow During Transition from Laminar to Turbulent Motion. Journal of Fluid Mechanics, Vol. 3, 1958, pp. 418-436.
6. Jaffe, N. A., Okamura, T. T., and Smith, A. M. O.: The Determination of Spatial Amplification Factors and Their Application to Predicting Transition. Preprint No. 69-10, AIAA, January 1969.
7. Favre, A. J.: The Equations of Compressible Turbulent Gases. Annual Summary Report No. 1, Institute de Mechanique Statistique de la Turbulence, January 1965.
8. Bradshaw, P. and Ferris, D. H.: Calculation of Boundary Layer Development Using the Turbulent Kinetic Energy Equation: Compressible Flow on Adiabatic Walls. Journal of Fluid Mechanics, Vol. 46, 1971, pp. 83-110.
9. McDonald, H. and Camarata, F. J.: An Extended Mixing Length Approach for Computing the Turbulent Boundary Layer Development. Proceedings of the AFOSR-IFP-Stanford Conference on Boundary Layer Prediction (Stanford, California), December 1968.

10. Glushko, G. S.: Turbulent Boundary Layer on a Flat Plate in an Incompressible Fluid. NASA TT F-10,800, 1965. Translation from Izvestiya Akademii Navk SSSR, Seriya Mekhanika, No. 4, pp. 13-23.
11. Donaldson, C duP., Sullivan, R. D., and Yates, J. E.: An Attempt to Construct an Analytical Model of the Start of Compressible Transition. Air Force Flight Dynamics Laboratory Technical Report TR-70-153, 1970.
12. McDonald, H. and Fish, R. W.: Practical Calculations of Transitional Boundary Layers. United Aircraft Research Laboratories Report No. L110887-1, March 1972.
13. Beckwith, I. E. and Bushnell, D. M.: Calculation of Mean and Fluctuating Properties of the Incompressible Turbulent Boundary Layer. Proceedings of the AFOSR-IFP-Stanford Conference on Turbulent Boundary Layer Prediction (Stanford, California), December 1968.
14. Dryden, H.: Transition from Laminar to Turbulent Flow. Turbulent Flow and Heat Transfer, Princeton University Press, Princeton, New Jersey, 1959, pp. 3-74.
15. Zysina-Molozhen, L. M. and Kuznetsova, V. M.: Investigation of Turbulent Conditions in a Boundary Layer. Thermal Engineering (Teploenergetika), Vol. 16, No. 7, 1969, pp. 16-20.
16. Wagner, R. D., Maddalon, D. V., and Weinstein, L. M.: Influence of Measured Free-Stream Disturbances on Hypersonic Boundary Layer Transition. AIAA Journal, Vol. 8, No. 9, September 1970, pp. 1664-1670.
17. Schubauer, C. G. and Tchen, C. M.: Turbulent Flow. Princeton University Press, Princeton, New Jersey, 1961.
18. Townsend, A. A.: Equilibrium Layers and Wall Turbulence. Journal of Fluid Mechanics, Vol. 11, 1961, pp. 97-120.
19. Bradshaw, P.: The Turbulence Structure of Equilibrium Boundary Layers. Journal of Fluid Mechanics, Vol. 29, 1967, pp. 625-645.
20. Coles, D. E.: The Turbulent Boundary Layer in a Compressible Fluid. Rand Report R403 PR, September 1962.

21. McDonald, H.: Mixing Length and Kinematic Eddy Viscosity in a Low Reynolds Number Boundary Layer. United Aircraft Research Laboratories Report J214453-1, September 1970.
22. Meier, H. V. and Rotta, J. C.: Experimental and Theoretical Investigations of Temperature Distribution in Supersonic Boundary Layers. Preprint No. 70-744, AIAA, 1970.
23. Rose, W. C.: Results of an Attempt to Generate a Homogeneous Turbulent Shear Flow. Journal of Fluid Mechanics, Vol. 25, 1967, pp. 97-120.
24. Shamroth, S. J. and Elrod, H. G.: The Development of the Reynolds Stress Tensor in a Turbulent Shear Flow. Journal of Basic Engineering, Vol. 92, 1970, pp. 836-842.
25. Maise, G. and McDonald, H.: Mixing Length and Eddy Kinematic Viscosity in a Compressible Boundary Layer. AIAA Journal, Vol. 6, January 1968, pp. 73-80.
26. Stalmach, C. J., Bertin, J. J., Pope, T. C., and McCloskey, M. H.: A Study of Boundary Layer Transition on Outgoing Gases in Hypersonic Flow. NASA CR-1908, 1971.
27. Laufer, J.: Sound Radiation from a Turbulent Boundary Layer. International Symposium on Mechanique de la Turbulence. Centre National de la Recherche Scientifique, Paris, France, 1962.
28. Stainback, P. C.: Hypersonic Boundary Layer Transition in the Presence of Wind-Tunnel Noise. AIAA Journal, Vol. 9, 1971, pp. 2475-2476.
29. Stainback, P. C., Fischer, M. C., and Wagner, R. D.: Effects of Wind Tunnel Disturbances on Hypersonic Boundary Layer Transition. Preprint No. 72-181, AIAA, January 1972.
30. Morkovin, M. V.: Critical Evaluation of Transition from Laminar to Turbulent Shear Layers with Emphasis on Hypersonically Traveling Bodies. Air Force Flight Dynamics Laboratory Report No. AFFDL-TR-68-149, 1969.
31. van Driest, E. R.: Convective Heat Transfer in Gases. Turbulent Flows and Heat Transfer, Ed. C. C. Lin, Princeton University Press, Princeton, New Jersey, 1959, pp. 339-427.

32. van Driest, E. R. and Boison, J. C.: Experiments on Boundary Layer Transition at Supersonic Speeds. Journal of the Aeronautical Sciences, Vol. 24, 1957, pp. 885-899.
33. Cary, A. M.: Turbulent Boundary Layer Heat Transfer and Transition Measurements for Cold Wall Conditions at Mach 6. AIAA Journal, Vol. 6, 1968, pp. 958-959.
34. Sanator, R. J., DeCarlo, J. P., and Torrillo, D. T.: Hypersonic Boundary Layer Transition Data for a Cold-Wall Slender Cone. AIAA Journal, Vol. 3, 1965, pp. 758-760.
35. Richards, B. E. and Stollery, J. L.: Further Experiments on Transition Reversal at Hypersonic Speeds. AIAA Journal, Vol. 4, 1966, pp. 224-226.
36. Sheetz, N. W.: Free Flight Boundary Layer Investigations at High Speeds. Preprint No. 65-127, AIAA, January 1965.
37. Higgins, R. W. and Pappas, C. C.: An Experimental Investigation of the Effect of Surface Heating on Boundary Layer Transition on a Flat Plate in Supersonic Flow. NACA TN 2351, 1951.
38. Cohen, N. B.: Boundary Layer Similar Solutions and Correlation Equations for Laminar Heat Transfer Distributions in Air at Velocities up to 41,100 Feet per Second. NASA TR R-118, 1961.
39. Holloway, P. F. and Sterrett, J. R.: Effect of Controlled Surface Roughness on Boundary Layer Transition and Heat Transfer at Mach Numbers of 4.8 and 6.0. NASA TN D-2054, 1964.
40. O'Donnell, R. M.: Experimental Investigation at a Mach Number of 2.41 of Average Skin Friction Coefficients and Velocity Profiles for Laminar and Turbulent Boundary Layers and an Assessment of Probe Effects. NACA TN 3122, 1954.
41. Michel, R. and Schmitt, V.: Resultats sur la Region de Transition de la Couche Limite en Hypersonique. L'Aeronautique et L'Astronautique, No. 19, March 1970, pp. 42-54.
42. Fischer, M. C. and Maddalon, D. V.: Experimental Laminar, Transitional, and Turbulent Boundary Layer Profiles on a Wedge at Local Mach Number 6.5 and Comparisons with Theory. NASA TN D-6462, September 1971.

43. Owen, F. K. and Horstman, C. C.: A Study of Hypersonic Transitional Boundary Layers. Paper presented at Boundary Layer Transition Workshop, San Bernadino, California, November 3-5, 1971.
44. Laufer, J.: The Structure of Turbulence in Fully Developed Pipe Flow. NACA TR 1174, 1952.
45. Kestler, A. L. and Chen, W. S.: The Fluctuating Pressure Field in a Supersonic Turbulent Boundary Layer. Journal of Fluid Mechanics, Vol. 16, 1963, pp. 41-64.
46. Fischer, M. C. and Weinstein, L. M.: Cone Transitional Boundary Layer Structure at $M_e = 14$. AIAA Journal, Vol. 10, No. 5, May 1972, pp. 699-701.
47. Beckwith, I. E. and Bertram, M. H.: A Survey of NASA Langley Studies on High Speed Transition and the Quiet Tunnel. NASA TMX2566, June 1972.
48. Richards, B. E.: Transitional and Turbulent Boundary Layers on a Cold Flat Plate in Hypersonic Flow. The Aeronautical Quarterly, Vol. 18, 1967, pp. 237-258.
49. Potter, J. L. and Whitfield, J. D.: Effect of Slight Nose Bluntness and Roughness on Boundary Layer Transition in Supersonic Flows. Journal of Fluid Mechanics, Vol. 12, 1962, pp. 501-535.
50. McCauly, W. D., Saydah, A. R., and Beuche, J. F.: Effects of Spherical Roughness on Hypersonic Boundary Layer Transition. AIAA Journal, Vol. 4, 1966, pp. 2142-2148.
51. Smith, A. M. O. and Clutter, D. W.: Solution of the Incompressible Boundary Layer Equations. AIAA Journal, Vol. 1, 1963, pp. 2062-2070.
52. Harvey, W. D., Bushnell, D. M., and Beckwith, I. E.: Fluctuating Properties of Turbulent Boundary Layers for Mach Numbers up to 9. NASA TN D-5496, October 1969.

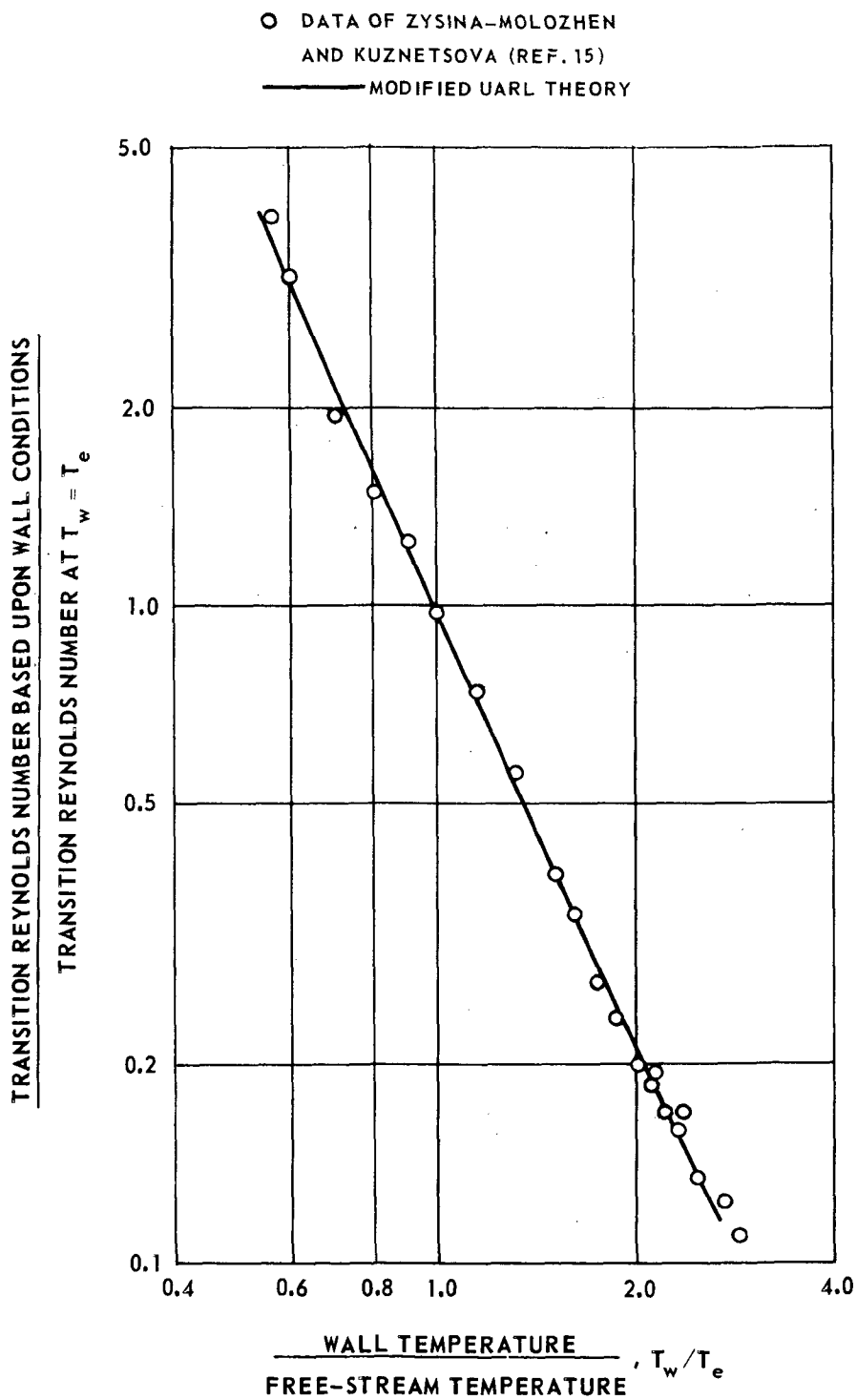


Figure1. — Variation of transition Reynolds number with wall temperature ratio for incompressible flow.

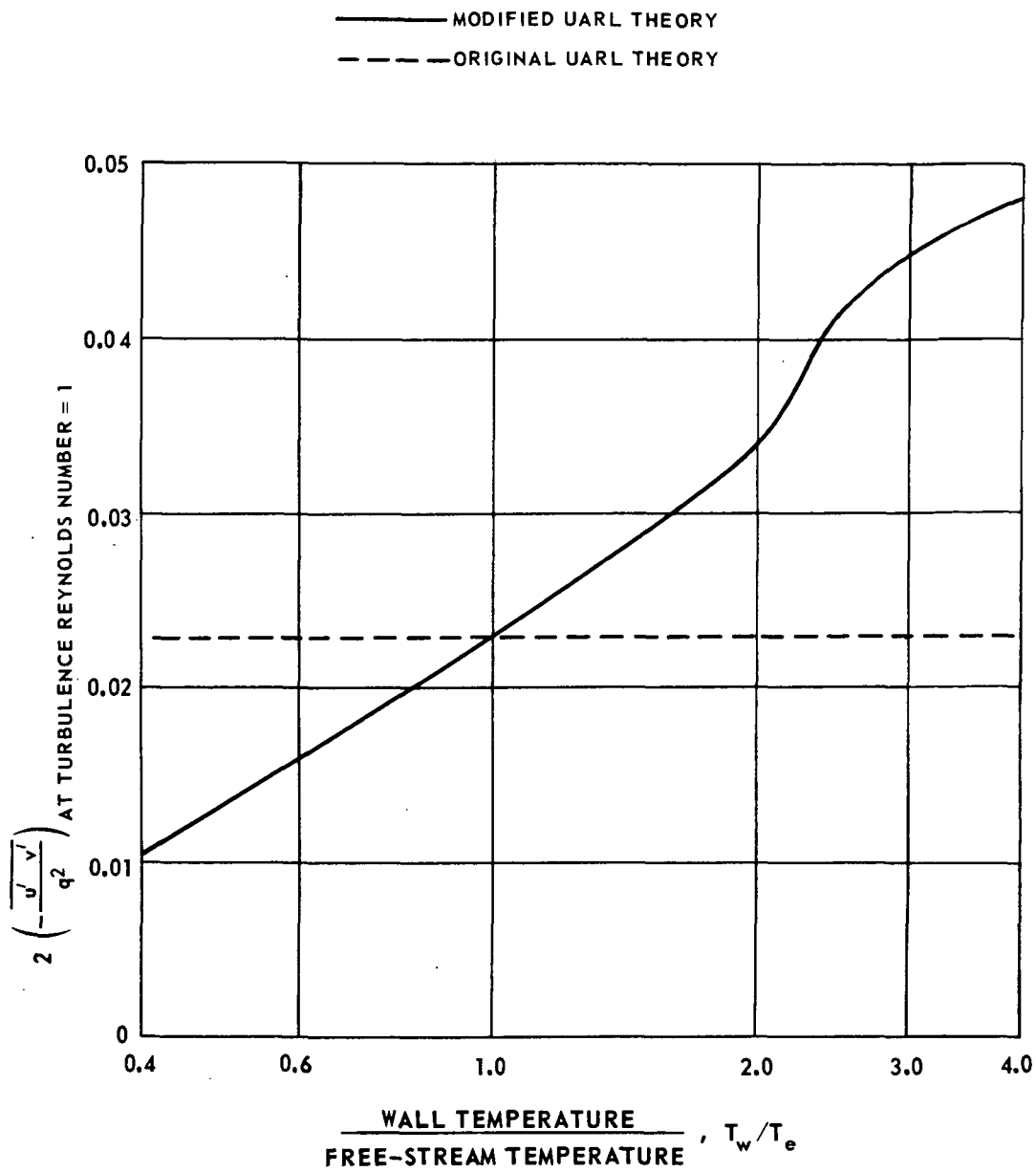


Figure 2. – Variation of structural coefficient with temperature ratio.

$$\left| \frac{u'}{u_e} \right| = \frac{K}{\gamma M_e M_r} \left| \frac{p'}{p_e} \right|$$

NASA DATA
(STAINBACK REF. 28)

ORIGINAL
UARL THEORY

MODIFIED
UARL THEORY

□

○

◇

--- {
K = 5.1
K = 9.8
K = 9.6

— K = 1.45

{
MACH 8 VARIABLE DENSITY TUNNEL
MACH 6 20" HYPERSONIC TUNNEL
MACH 6 HIGH REYNOLDS
NUMBER TUNNEL

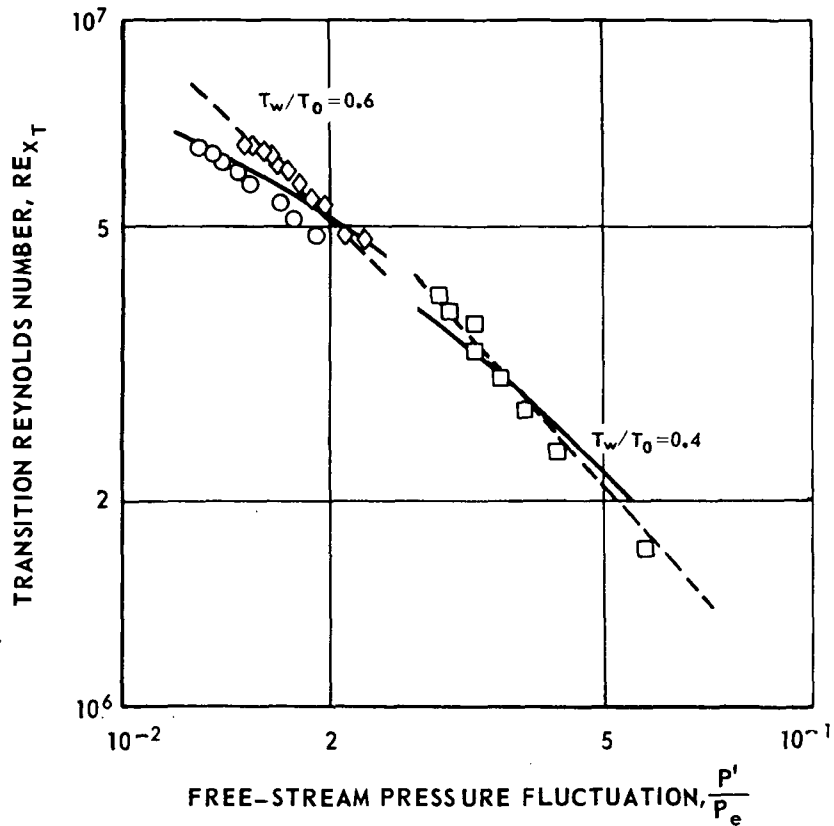


Figure 3. - Effect of free-stream fluctuating pressure on boundary layer transition location on sharp cones at $M_e = 5$.

—●— LAMINAR THEORY (REF. 38)

— MODIFIED UARL THEORY

STAINBACK'S DATA (REF. 29) - 20 IN. HYPERSONIC TUNNEL

$M_\infty = 6.0, M_e = 5.0$

○ St_{LAMINAR}

□ $St_{\text{TURBULENT}}$

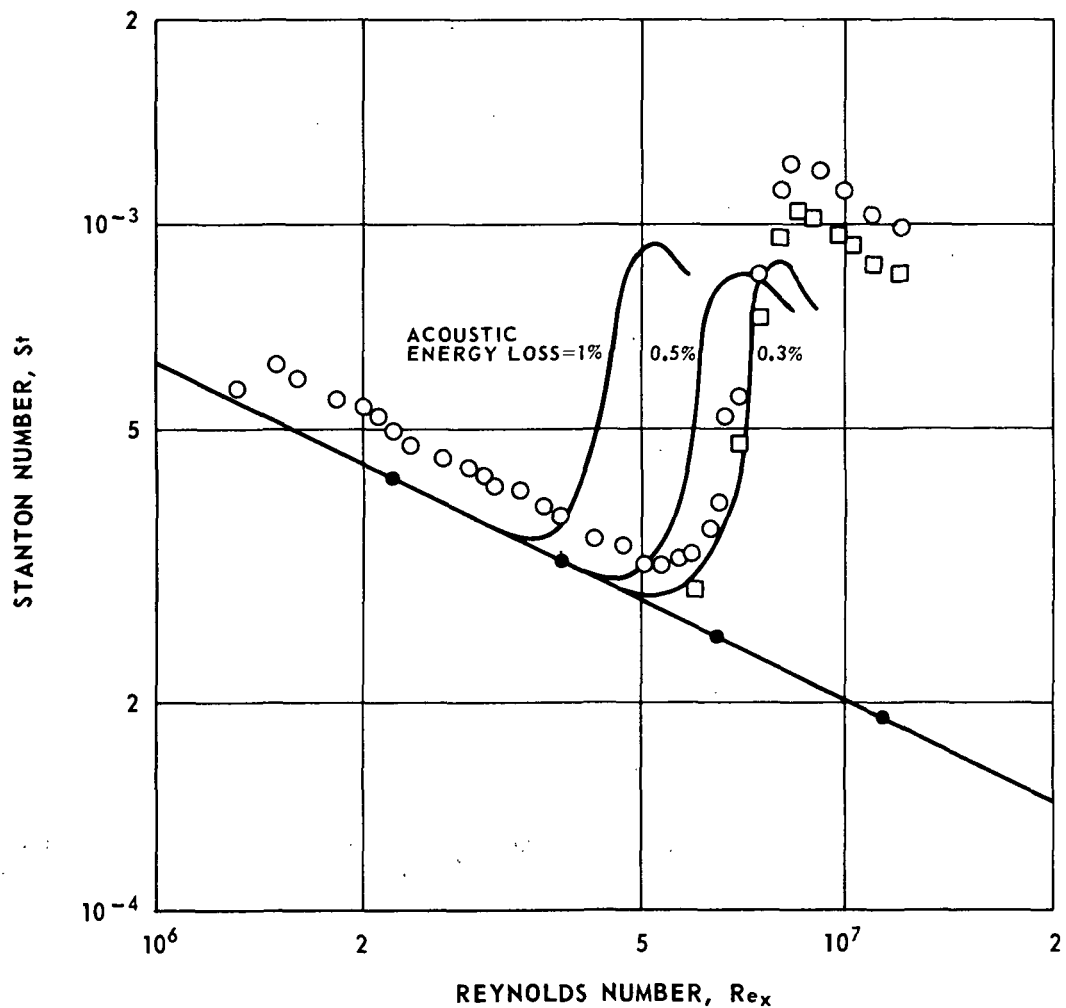


Figure 4. - Comparison between measured and predicted transitional heat transfer with transition triggered from pressure - velocity fluctuation.

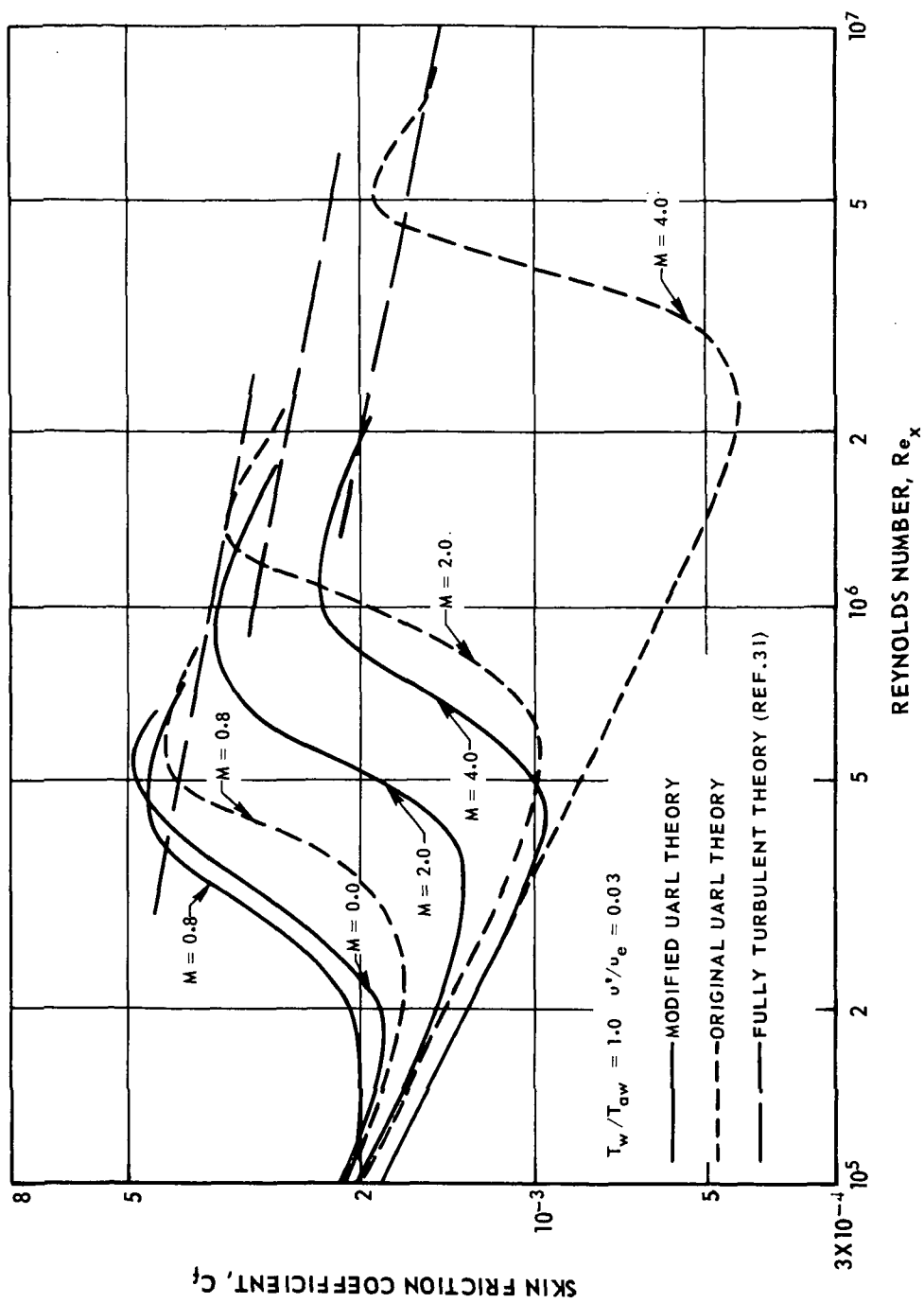


Figure 5. — Predicted variation of transitional skin friction for various Mach numbers.

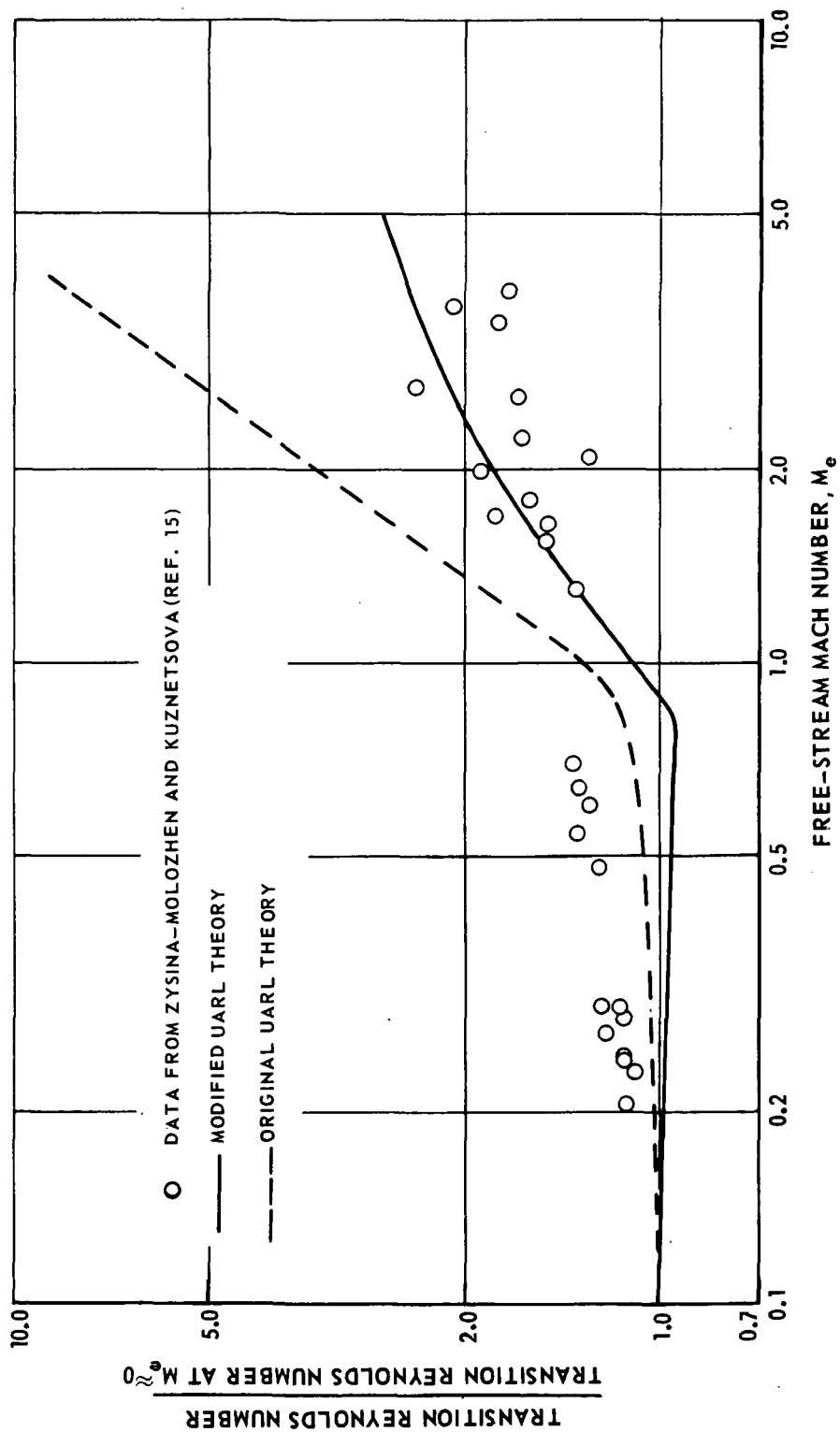


Figure 6. — Variation of transition Reynolds number with Mach number.

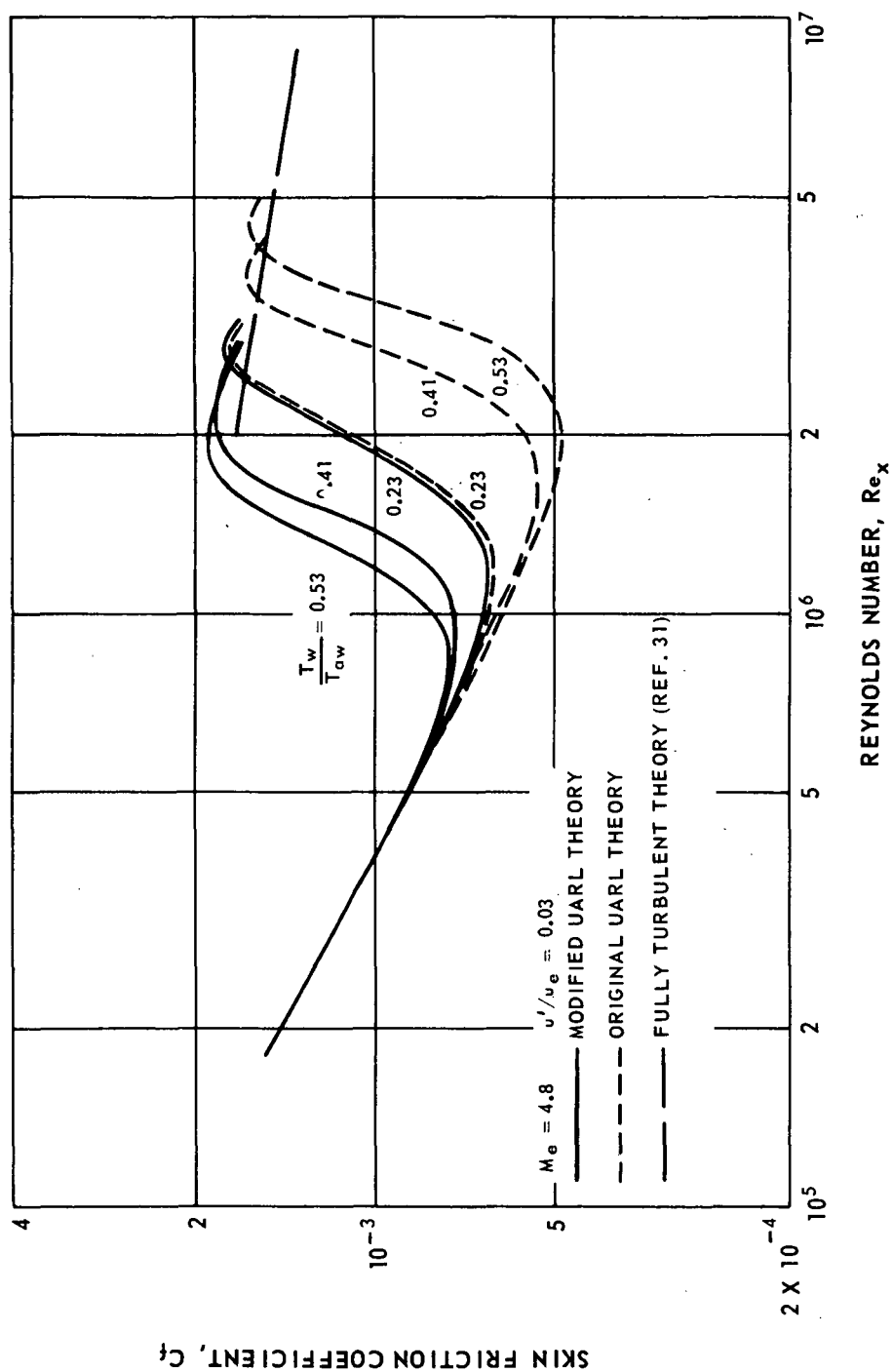


Figure 7. — Predicted variation of transitional skin friction for various wall temperature ratios.

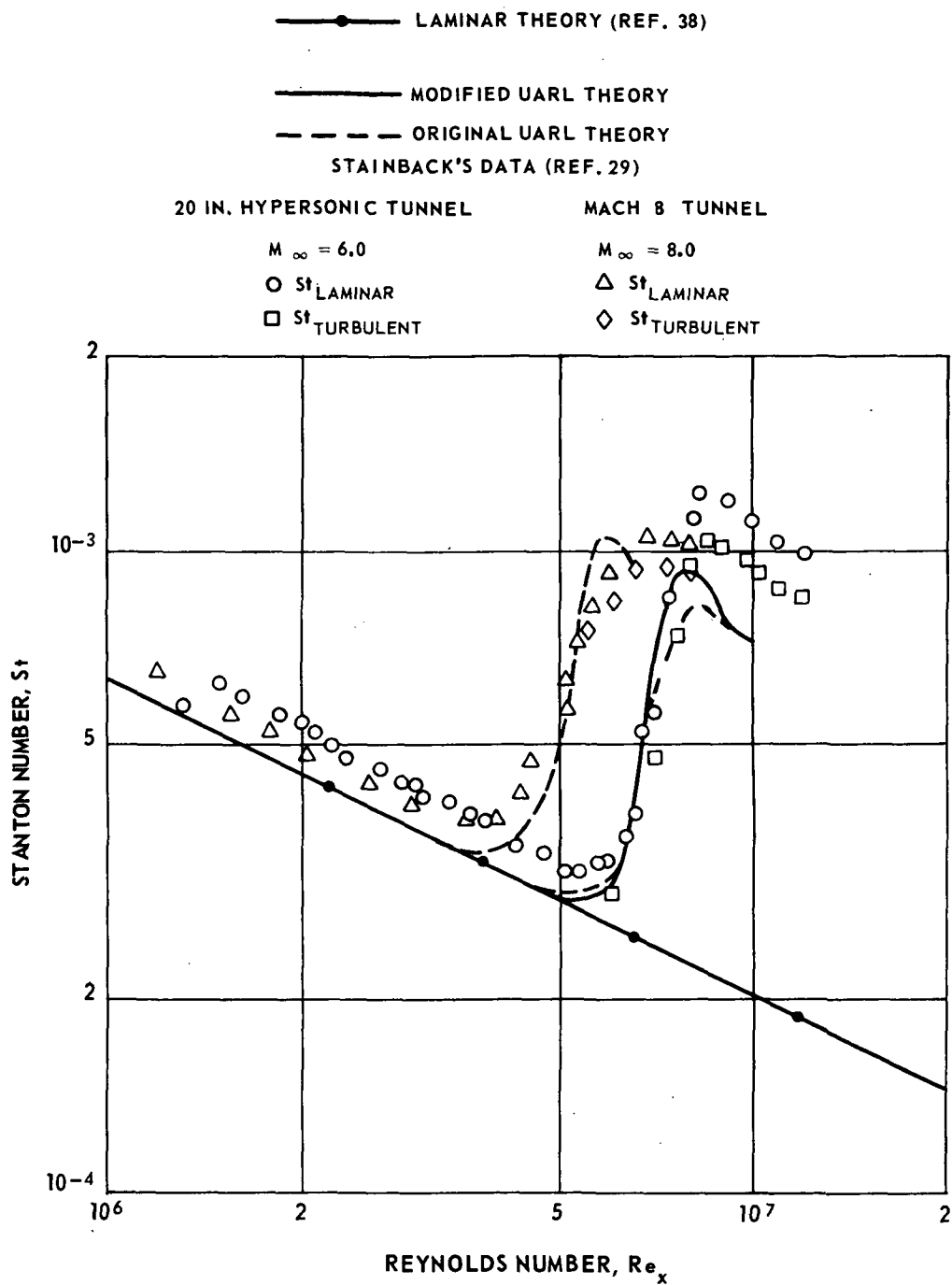


Figure 8. — Comparison between measured and predicted transitional heat transfer at $Me = 5$.

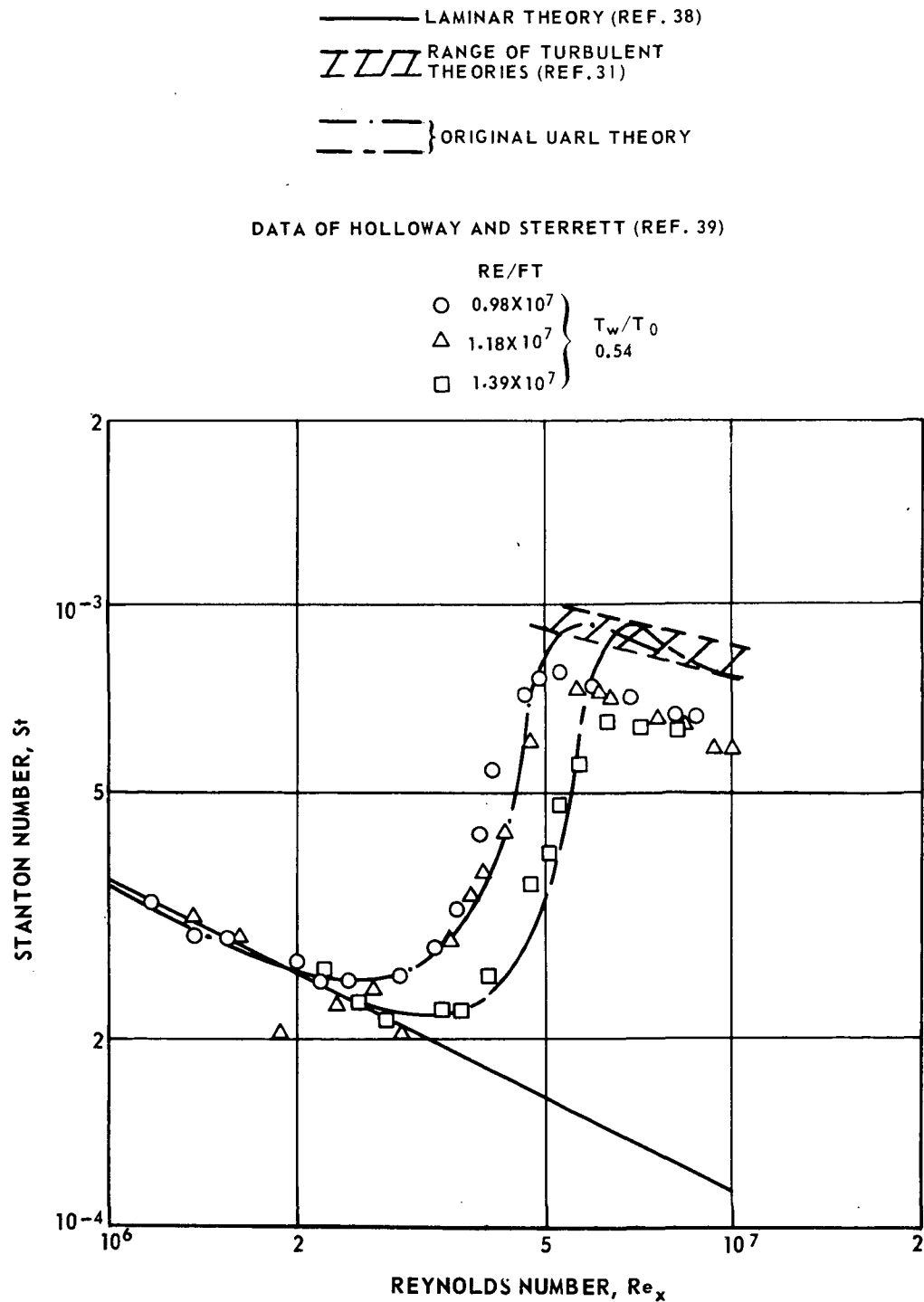


Figure 9. — Comparison between measured and predicted transitional heat transfer at $Me = 4.8$.

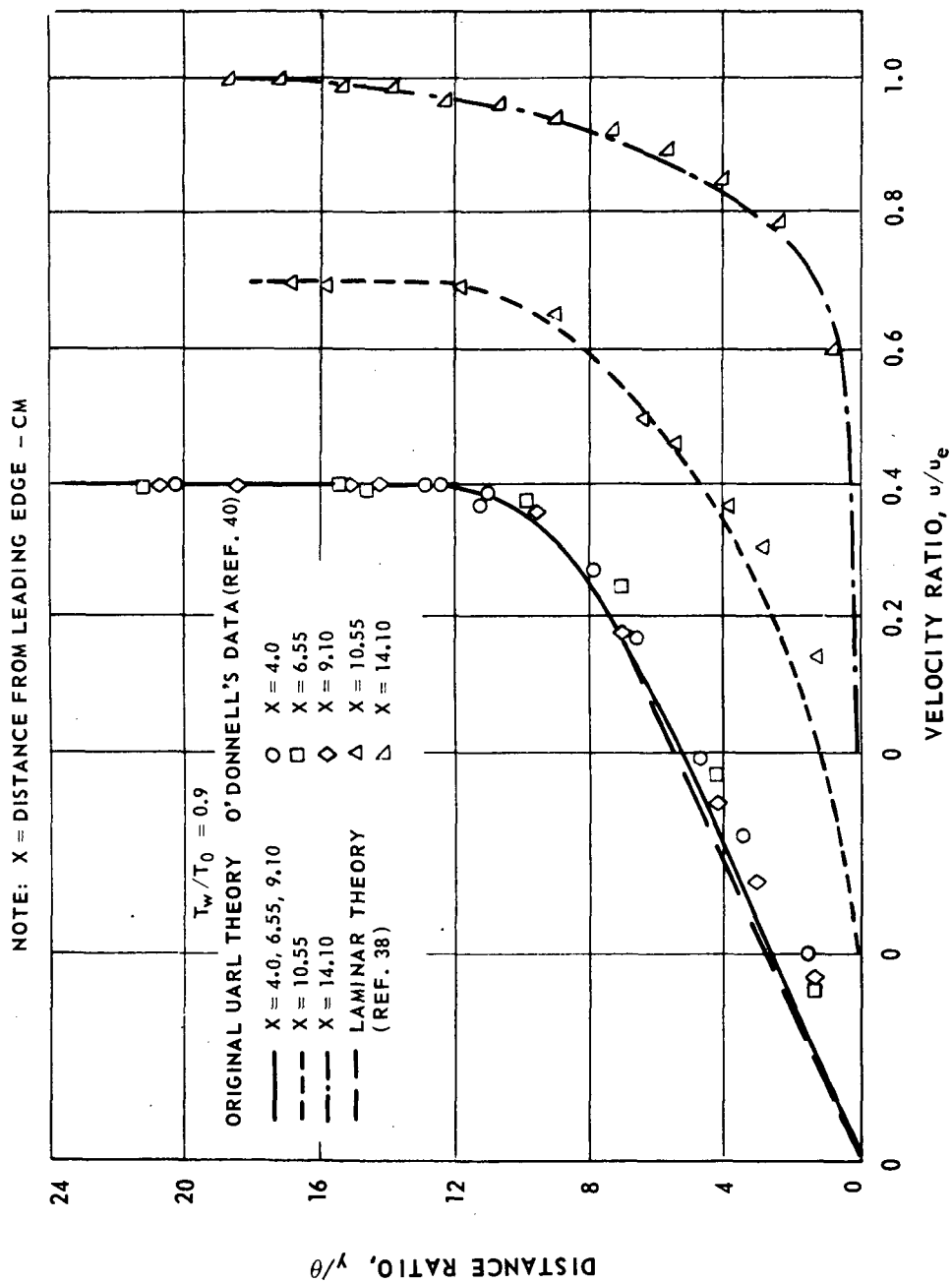


Figure 10. — Comparison between measured and predicted transitional velocity profiles at $Me = 2.4$.

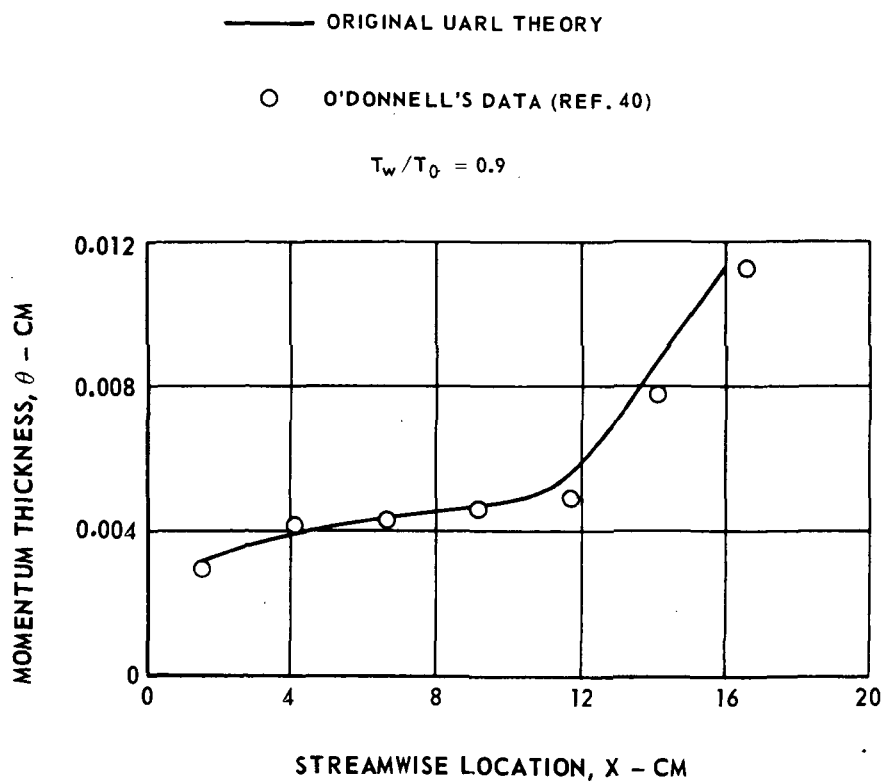


Figure 11. - Comparison between measured and predicted momentum thickness at $M_e = 2.4$.

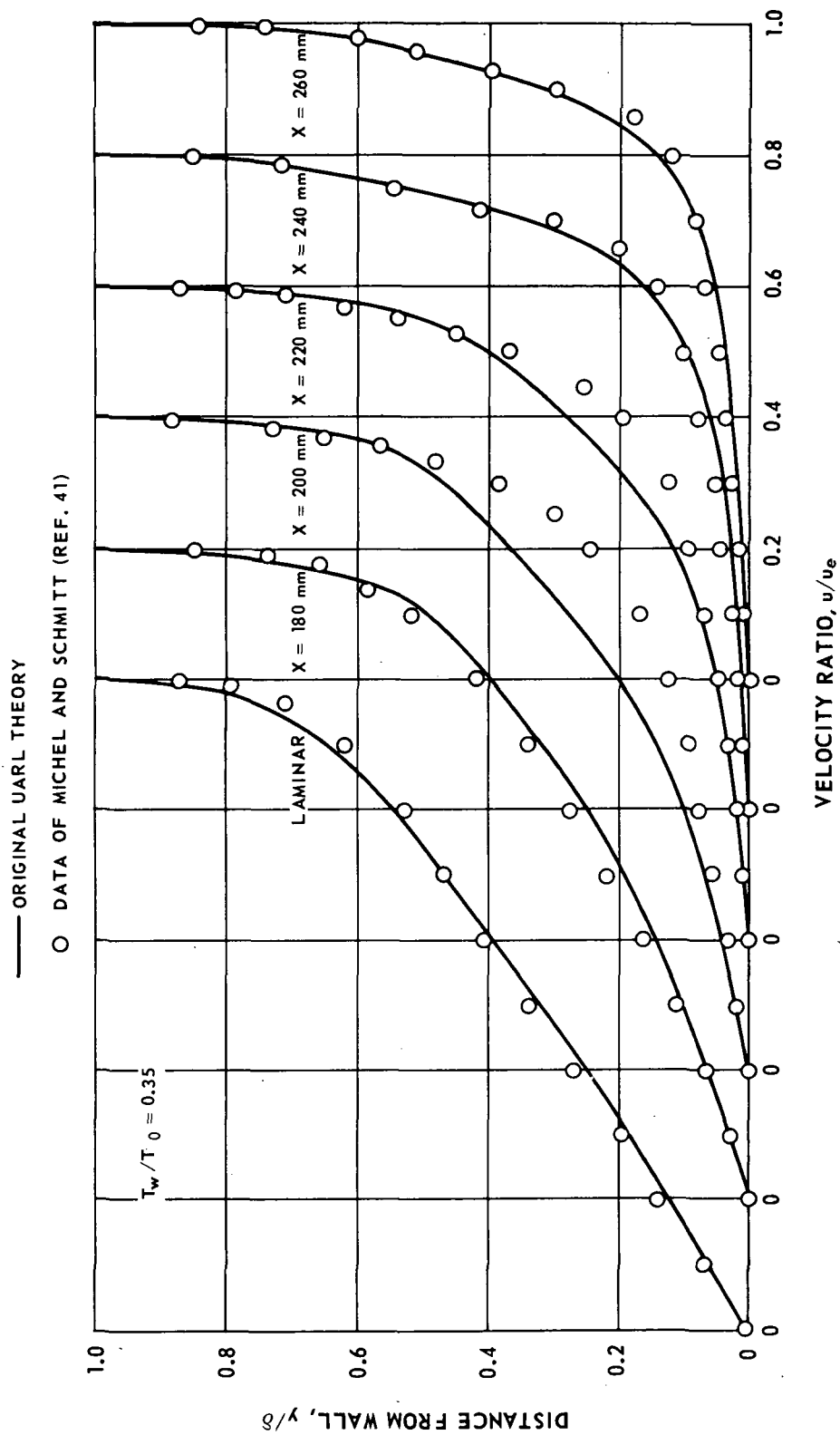


Figure 12. — Comparison between measured and predicted transitional velocity profiles at $Me = 6.6$.

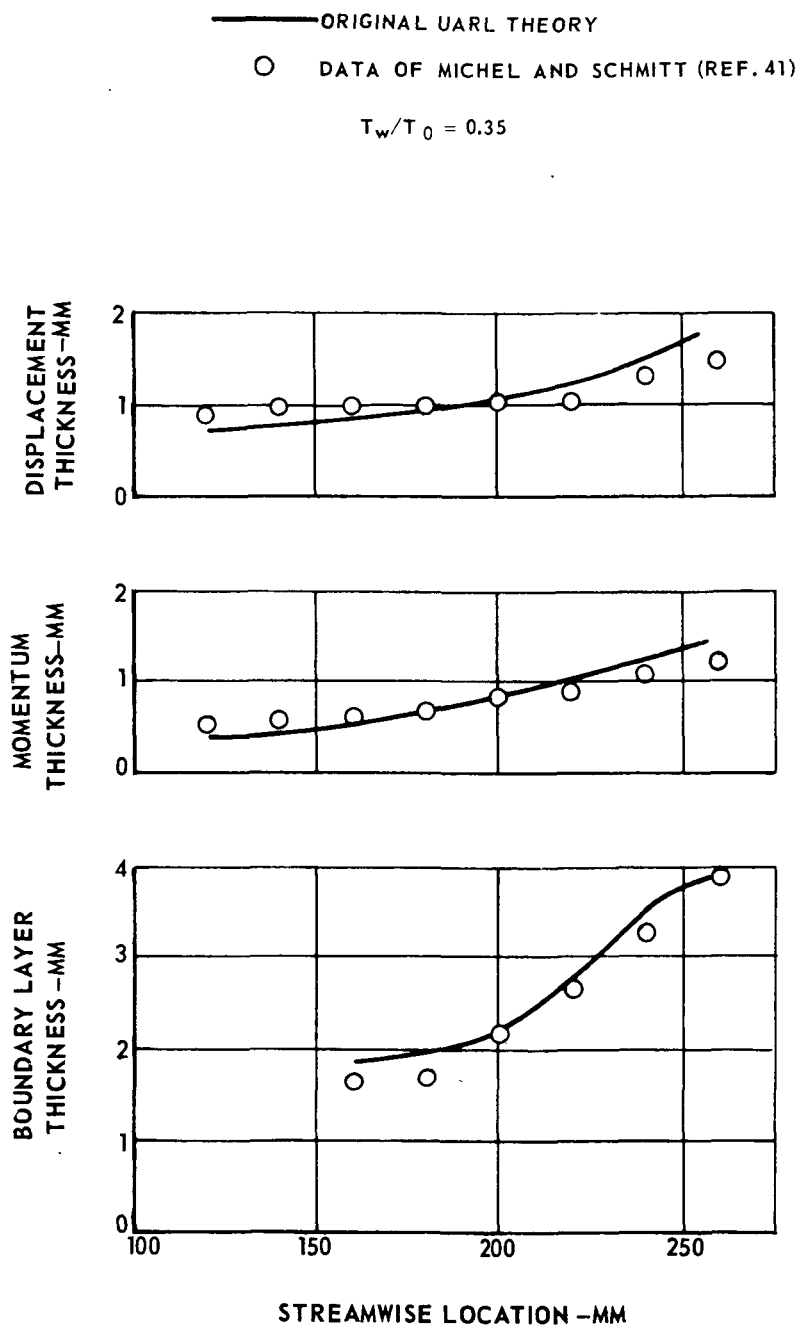


Figure 13. – Comparison between measured and predicted variation of boundary layer integral parameters through transition at $M_e = 6.6$.

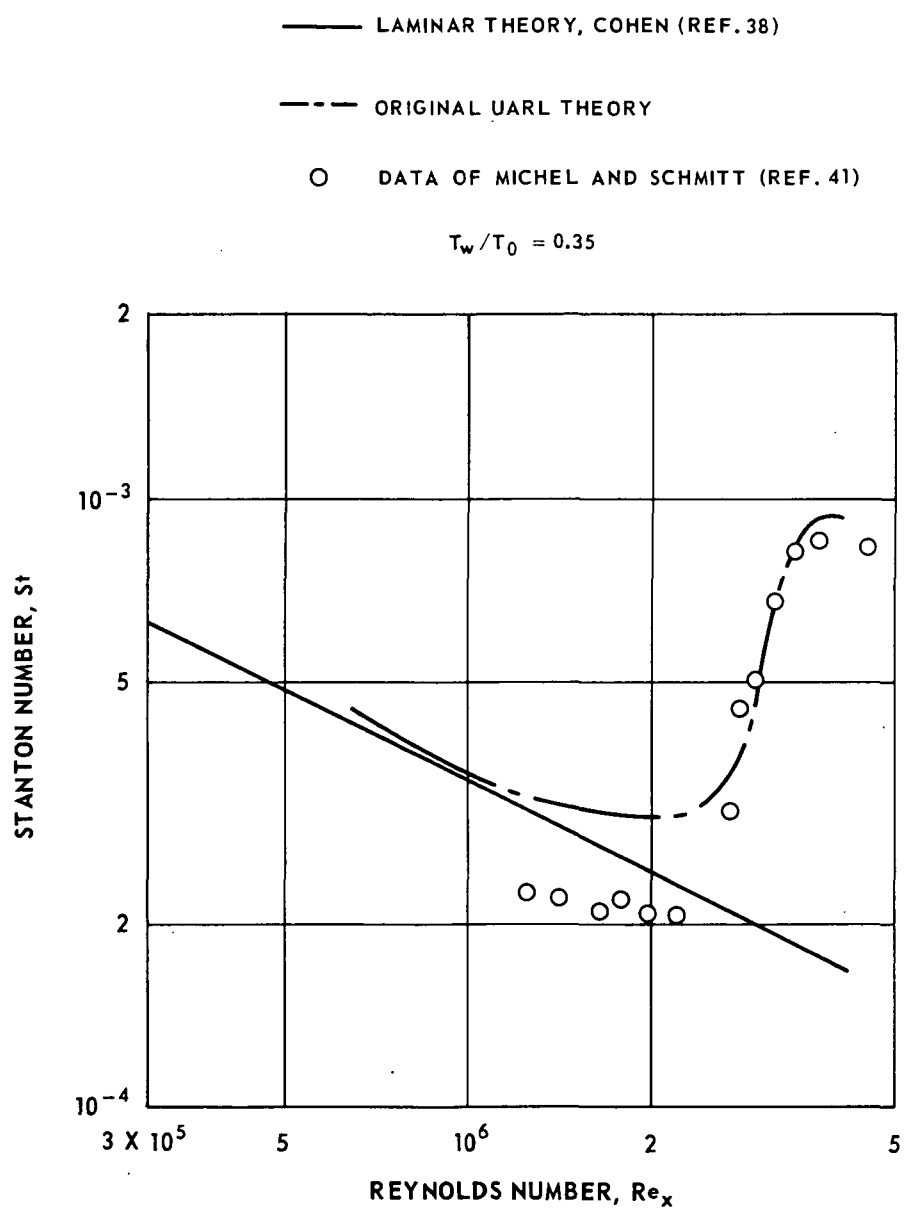


Figure 14. — Comparison between measured and predicted transitional heat transfer at $M_e = 6.6$.

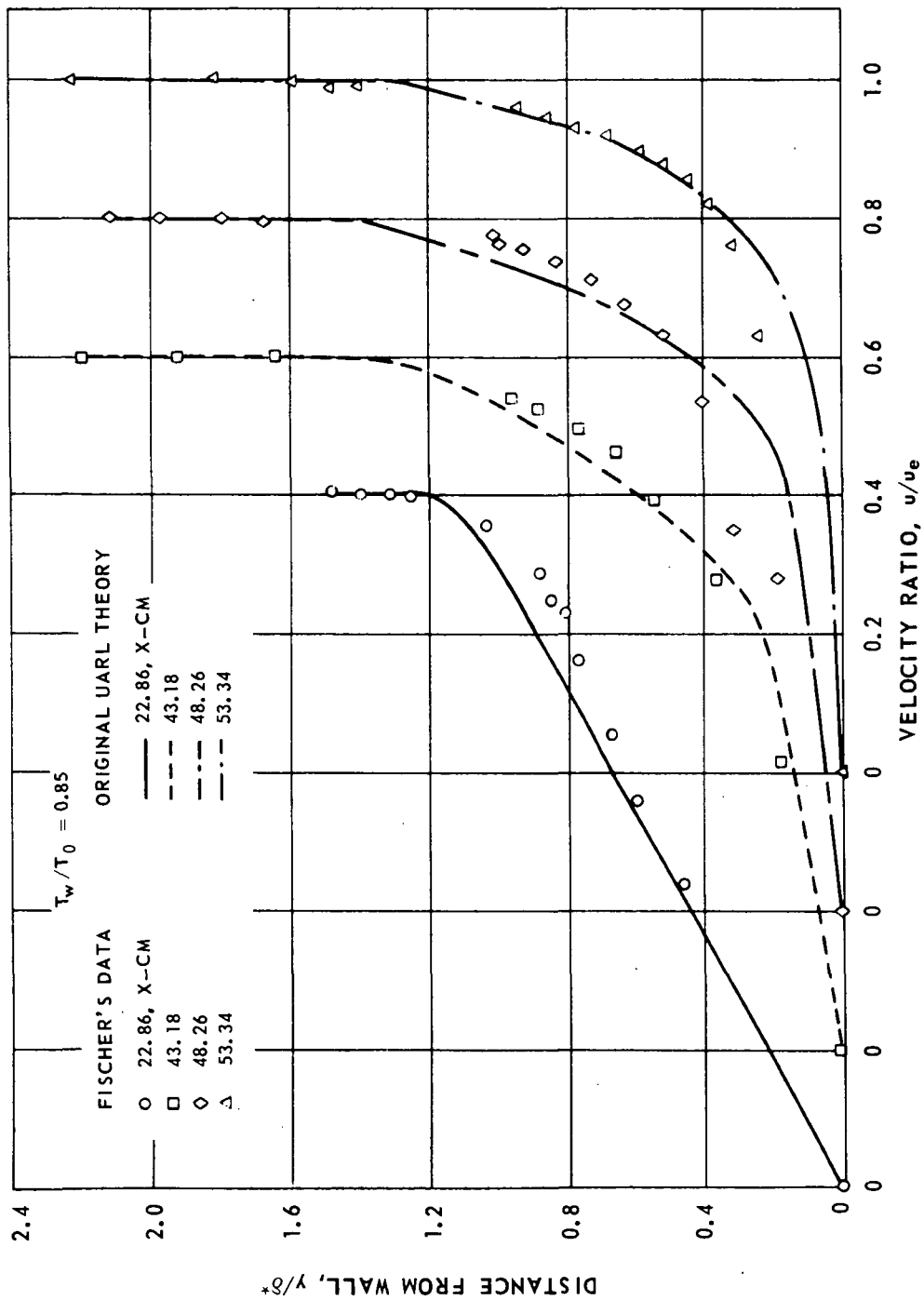


Figure 15. — Comparison between measured and predicted transitional velocity profiles at $M_e = 6.2$.

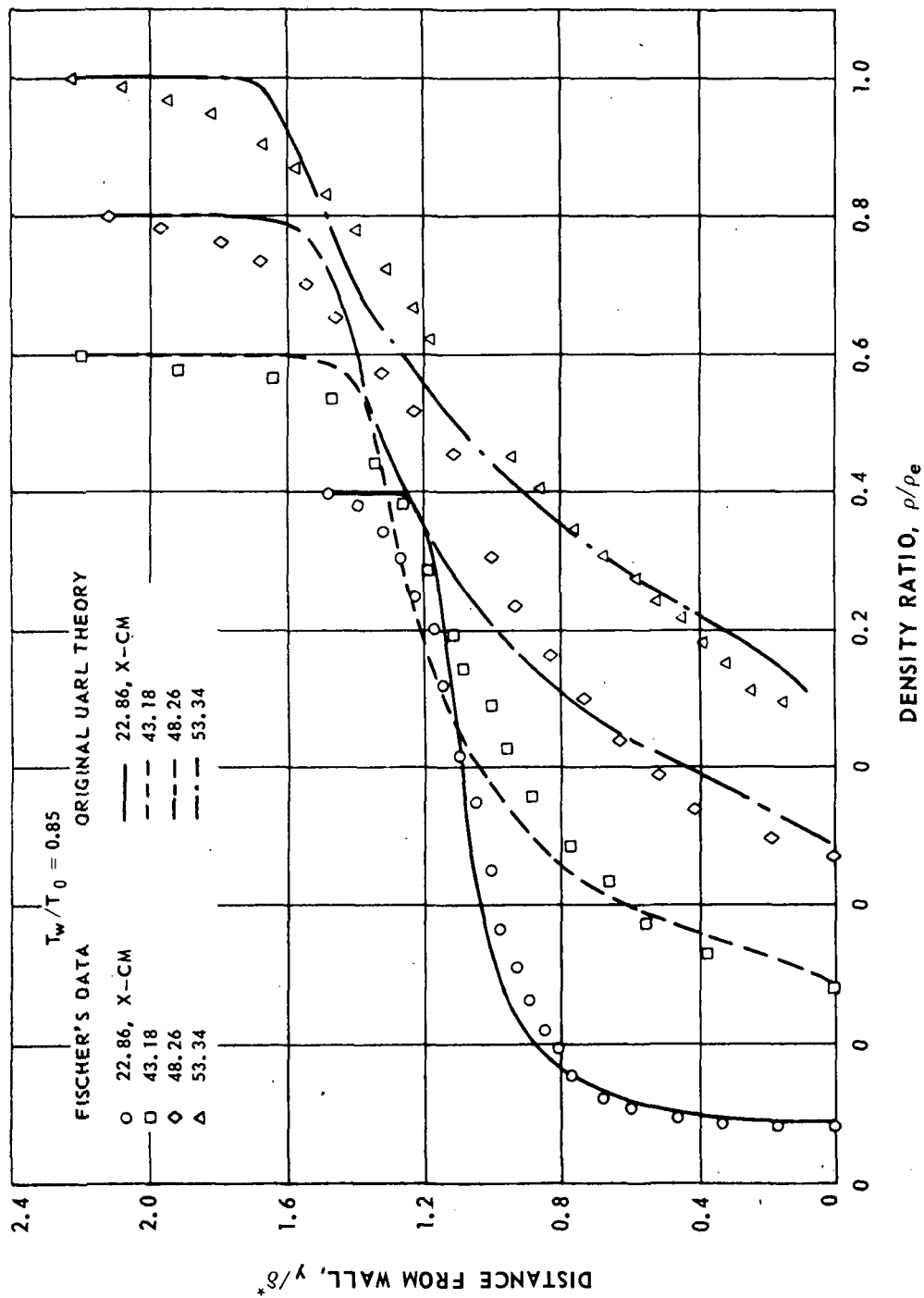


Figure 16. — Comparison between measured and predicted transitional density profiles at $M_e = 6.2$.

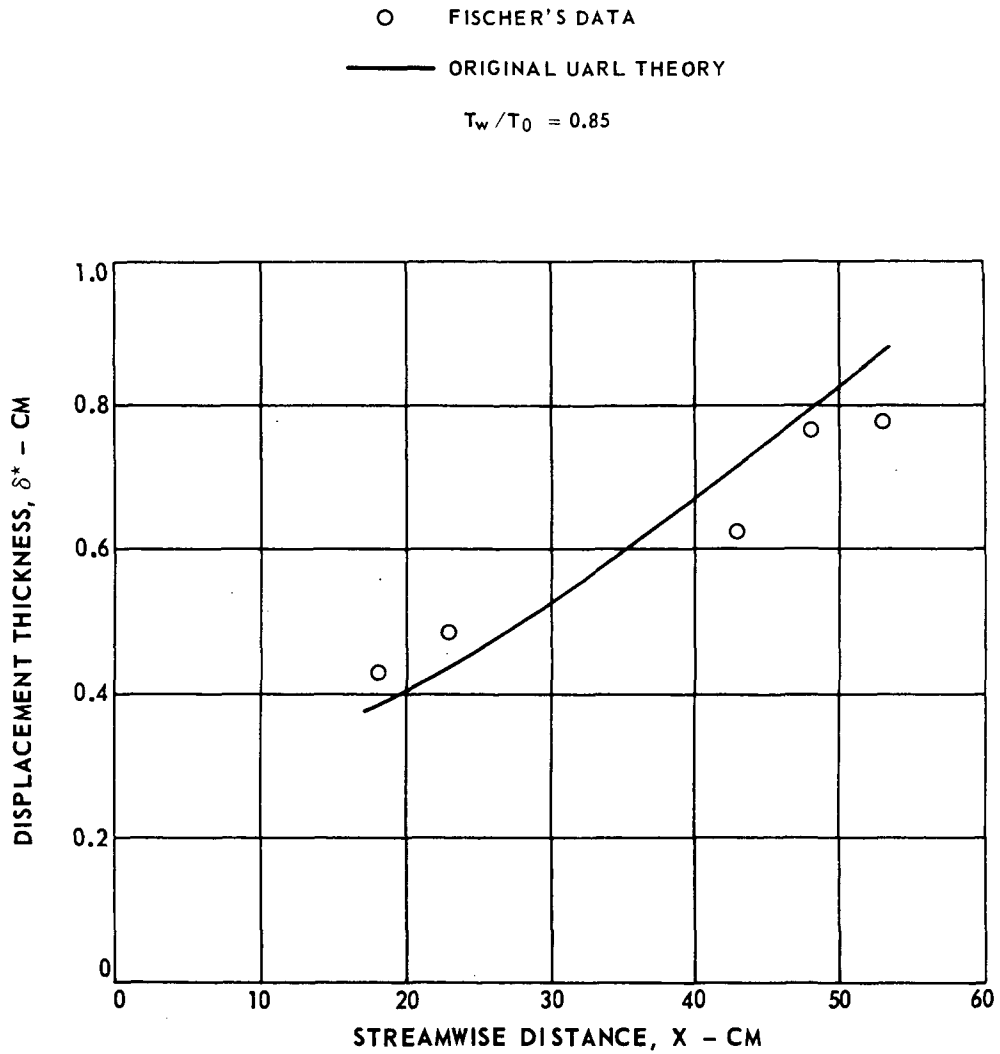


Figure 17. — Comparison between measured and predicted variation of displacement thickness through transition at $M_e = 6.2$.

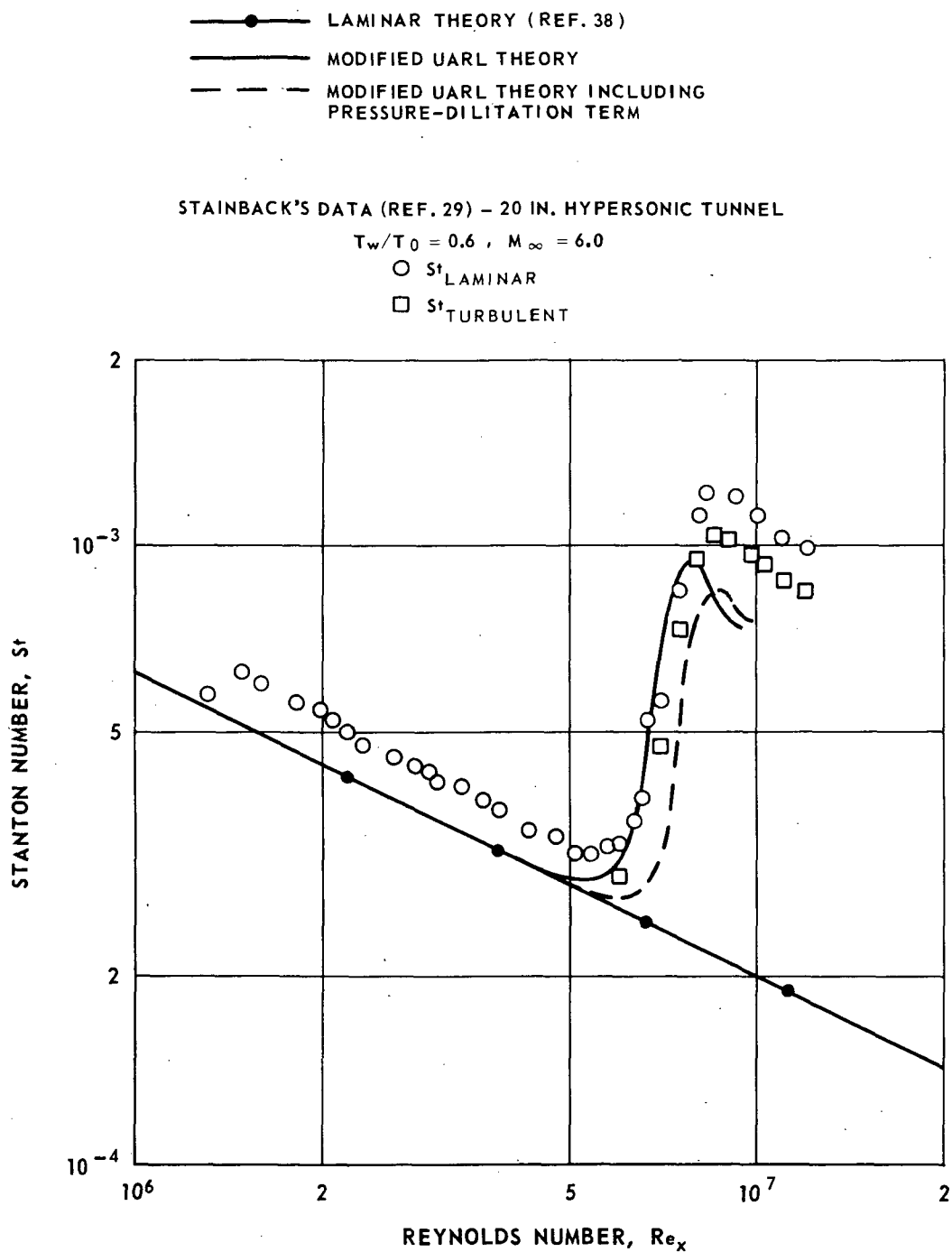


Figure 18. - Comparison between measured and predicted transitional heat transfer at $M_e = 5$.

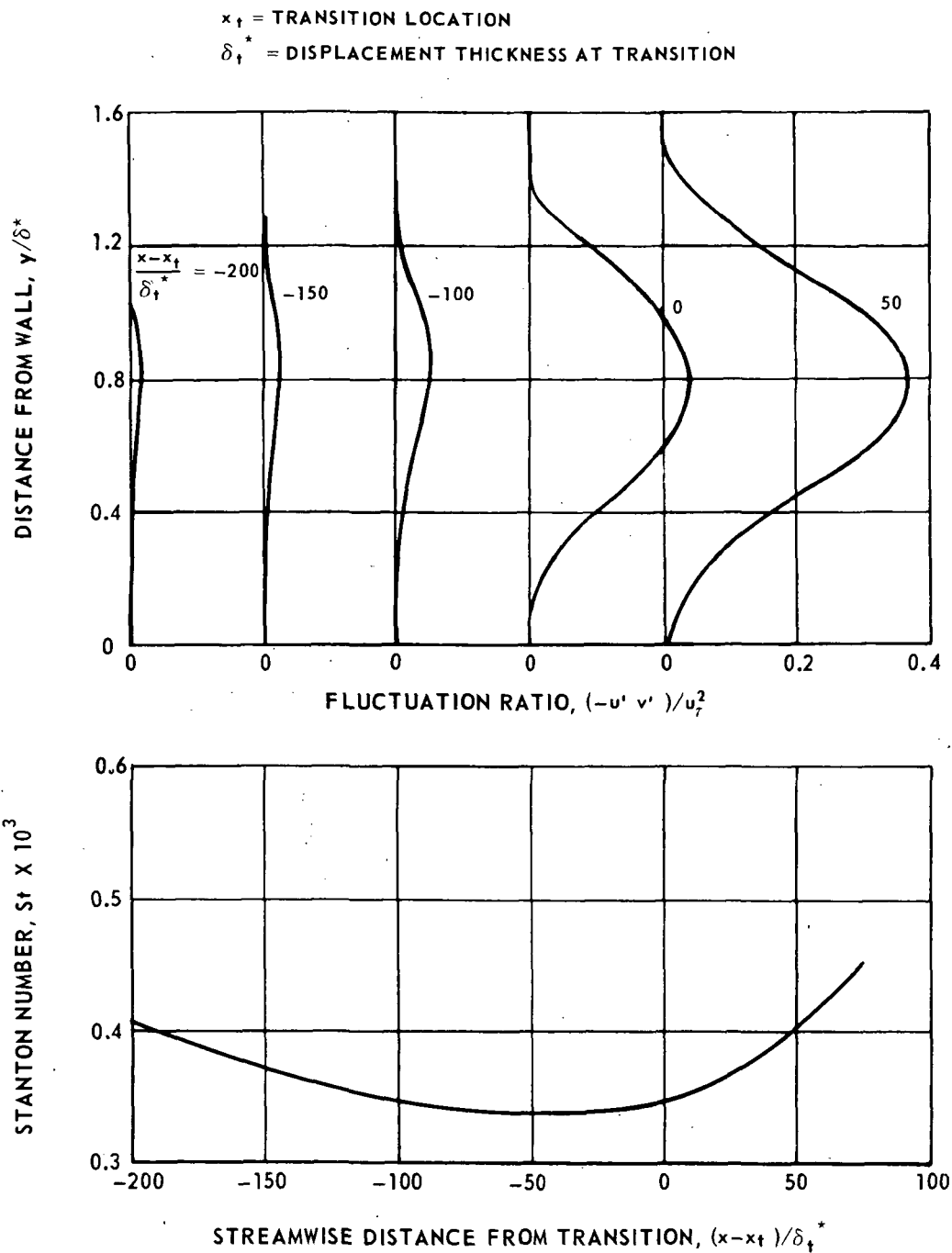


Figure 19. - Reynolds stress profiles upstream of transition.



POSTMASTER :

If Undeliverable (Section 158
Postal Manual) Do Not Return

"The aeronautical and space activities of the United States shall be conducted so as to contribute . . . to the expansion of human knowledge of phenomena in the atmosphere and space. The Administration shall provide for the widest practicable and appropriate dissemination of information concerning its activities and the results thereof."

—NATIONAL AERONAUTICS AND SPACE ACT OF 1958

NASA SCIENTIFIC AND TECHNICAL PUBLICATIONS

TECHNICAL REPORTS: Scientific and technical information considered important, complete, and a lasting contribution to existing knowledge.

TECHNICAL NOTES: Information less broad in scope but nevertheless of importance as a contribution to existing knowledge.

TECHNICAL MEMORANDUMS: Information receiving limited distribution because of preliminary data, security classification, or other reasons. Also includes conference proceedings with either limited or unlimited distribution.

CONTRACTOR REPORTS: Scientific and technical information generated under a NASA contract or grant and considered an important contribution to existing knowledge.

TECHNICAL TRANSLATIONS: Information published in a foreign language considered to merit NASA distribution in English.

SPECIAL PUBLICATIONS: Information derived from or of value to NASA activities. Publications include final reports of major projects, monographs, data compilations, handbooks, sourcebooks, and special bibliographies.

TECHNOLOGY UTILIZATION PUBLICATIONS: Information on technology used by NASA that may be of particular interest in commercial and other non-aerospace applications. Publications include Tech Briefs, Technology Utilization Reports and Technology Surveys.

Details on the availability of these publications may be obtained from:

SCIENTIFIC AND TECHNICAL INFORMATION OFFICE

NATIONAL AERONAUTICS AND SPACE ADMINISTRATION

Washington, D.C. 20546